

How cytoskeleton senses abiotic/biotic stimuli in plant cells?

Zur Erlangung des akademischen Grades eines

DOKTORS DER NATURWISSENSCHAFTEN

(Dr. rer. Nat.)

der Fakultät für Chemie und Biowissenschaften
des Karlsruher Instituts für Technologie (KIT)

vorgelegte

Dissertation

von

Fei Qiao

aus Shaanxi, China

die vorliegende Dissertation wurde am Botanischen Institut des Karlsruhe Instituts für Technologie (KIT), Lehrstuhl 1 für Molekulare Zellbiologie, im Zeitraum von Dezember 2007 bis Juni 2010 angefertigt.

Dekan: Prof. Dr. Stefan Bräse

Referent: Prof. Dr. Peter Nick

Korreferent: Prof. Dr. Martin Bastmeyer

Tag der mündlichen Prüfung: 12 Juli, 2010

Hiermit erkläre ich, dass ich die vorliegende Dissertation, abgesehen von der Benutzung der angegebenen Hilfsmittel, selbständig verfasst habe.

Alle Stellen, die gemäß Wortlaut oder Inhalt aus anderen Arbeiten entnommen sind, wurden durch Angabe der Quelle als Entlehnungen kenntlich gemacht.

Diese Dissertation liegt in gleicher oder ähnlicher Form keiner anderen Prüfungsbehörde vor.

Karlsruhe, den 10. Mai 2010

Fei Qiao

Content

A List of Abbreviations.....	IV
Zusammenfassung	VI
1 Introduction	1
1.1 Functions of cytoskeleton in plant cell morphogenesis	2
1.1.1 Roles of cytoskeleton in cell expansion and cell wall formation.....	2
1.1.2 Microtubule and cell division axis	4
1.2 Types of signal-triggered cytoskeletal responses	5
1.2.1 Reorientation	6
1.2.2 Disorganization/Disassembly.....	7
1.2.3 Bundling	8
1.2.4 Post-translational modifications	9
1.3 The plant cytoskeleton in sensing of abiotic signals	11
1.3.1 Function of microtubules in response to abiotic stimuli.....	11
1.3.2 Functions of microfilaments in response to abiotic stimuli	14
1.3.3 Actin, auxin, light and synchronized division patterns.....	15
1.4 The plant cytoskeleton in sensing of biotic signals	17
1.4.1 Cytoskeletal responses during host-pathogen interaction-How can a plant recognize and defend itself against pathogens?.....	17
1.4.2 Elicitors triggered defence responses in plants	20
1.5 Dose cytoskeleton act upstream in signal transduction?.....	21
1.5.1 Cytoskeleton acts as a sensor or a regulator?.....	22
1.5.2 Cytoskeleton acts as a transducer?.....	22
1.6 Approaches of this study.....	23
1.6.1 Cytoskeletal responses to light in synchronized cell division pattern.....	23
1.6.2 Role of cytoskeleton in response to the Harpin elicitor in grapevine.....	25
2 Materials and Methods.....	27
2.1 Cell lines	27
2.2 NPA and auxin treatments.....	28

2.3 Quantification of pattern and morphology	28
2.4 Light sources and irradiation	28
2.5 pH measuring and recording	29
2.6 Microtubule visualization and quantitative analysis	29
2.7 Visualization of actin microfilaments	31
2.8 RNA isolation and RT-PCR.....	32
2.9 Determination of cell viability	33
2.10 Protein extraction and western blot analysis.....	34
2.11 Quantification of growth response to oryzalin.....	35
2.12 Programmed cell death detection	35
3 Results	37
3.1 Light can rescue auxin-dependent synchrony of cell division in a tobacco cell line.....	37
3.1.1 Cell division pattern of VBI-3	37
3.1.2 The synchrony of cell division is affected by NPA and can be rescued by light or IAA.....	39
3.1.3 The rescue of the division synchrony by light depends on light quality.....	41
3.1.4 NPA affects the organization of actin filaments	43
3.1.5 Summary	44
3.2 Cytoskeleton acts upstream of the gene expression in response to the Harpin elicitor in grapevine	44
3.2.1 Harpin induces extracellular alkalization	45
3.2.2 Harpin induces microtubule disintegration	47
3.2.3 Harpin induces actin bundling.....	51
3.2.4 Harpin induces defence-related genes	53
3.2.5 Cytoskeletal compounds induce RS and StSy in the absence of elicitor	56
3.2.6 The effect of Harpin on induction of cell death.....	58
3.2.7 Summary	59
4 Discussion.....	61
4.1 Synchronized cell division is under the control of polar auxin	

Content

transport.....	61
4.1.1 Light reverses the effect of NPA on synchronized division.....	62
4.1.2 Phytochrome A is involved in the light dependent rescue.....	63
4.2 The differences of defense response in resistant and sensitive grapevine species	67
4.2.1 Defence responses triggered by Harpin are more profound and rapid in resistant species	68
4.2.2 Two grapevine cell line undergo different microtubular disintegration in response to Harpin	69
4.3 Differential response of the plant cytoskeleton during the sensing of light and elicitor	70
4.4 Conclusion	72
5 Outlook.....	74
Acknowledgements.....	76
Literature cited	77
Curriculum Vitae	88

A List of Abbreviations

2,4-D, 2,4-dichlorophenoxyacetic acid

ADF, actin depolymerising factor

AF, actin filament

BSA, bovine serum albumin

BY-2, tobacco cell line L. cv. Bright-Yellow 2

cMTs, cortical microtubules

DIC, differential interference contrast

DMSO, dimethyl sulfoxide

EC, effective concentration

FITC, Fluorescein isothiocyanate

HR, hypersensitive response

IAA, Indolyl-3-acetic acid

Lat B, latrunculin B

M, molar (mole /liter)

MF, microfilament

MS, Murashige and Skoog medium

Abbreviation

MT, microtubule

NAA, 1-naphthaleneacetic acid

NPA, 1- naphthylphthalamic acid

OGs, oligogalacturonides

PAMPs, pathogen-associated molecular patterns

PBS, phosphate buffered saline

PCD, programmed cell death

PPB, preprophase band

ROS, reactive oxygen species

RT-CR, reverse transcription polymerase chain reaction

rpm, rounds per minute

SE, standard error

Tris, tris(hydroxymethyl)-aminomethane

TTSS, type three secretion system

VBI-3, tobacco cell line

L. cv. Virginia Bright Italia 3

v/v, volume per volume

w/v, weight per volume

Zusammenfassung

In der vorliegenden Arbeit wurde die Funktion des Cytoskeletts in der Perzeption von biotischen und abiotischen Reizen untersucht. Als Indikator der zellulären Antwort wurde die Synchronität der Zellteilung gewählt, während als biotischer Reiz ein durch einen simulierter Pathogenbefall und als abiotischer Reiz Licht genutzt wurde. Die Ergebnisse zeigen eine unterschiedliche Antwort des Cytoskeletts auf diese beiden Reize hinsichtlich Reorganisation und Signaltransduktion.

Die Synchronität der Zellteilung kann durch den Inhibitor des Auxintransports NPA unterdrückt werden. Dieser Prozess wird begleitet von der Deassemblierung der Aktinfilamente. In der auf Licht reagierenden und Auxin-unabhängigen Tabak-Zelllinie VBI-3 kann diese Antwort durch Kultur im Licht oder durch Zugabe von exogener IAA rückgängig gemacht werden. Die kontinuierliche Bestrahlung mit dunkelrotem Licht stellte die Synchronität der Zellteilung am effektivsten wieder her. Wir nehmen an, dass Licht die Synchronität der Zellteilung durch Phytochrom-vermittelte Auxin-Biosynthese und Mikrofilament-abhängigen Auxintransport beeinflusst. Die Ergebnisse zeigen, dass Mikrofilamente als Bindeglied zwischen Lichtreiz und Musterbildung fungieren.

Der Harpin löst verschiedene Abwehrreaktionen aus. Hierzu gehören extrazelluläre Alkalisierung, Bündelung von Mikrofilamenten, Zerfall von Mikrotubuli und die Genexpression von Abwehr-Genen in cv. 'Pinot Noir' und . Diese Abwehrreaktionen waren durchweg schneller und deutlicher in Der höhere Gehalt an detyrosiniertem Tubulin fördert in die Stabilität des Mikrotubuli-Netzwerks, was darauf hinweist, dass Mikrotubuli ein mögliches Ziel des Pathogenbefalls sind. Inhibitoren des Cytoskeletts können zum Teil die gleichen Effekte wie der auslösen. Wir ziehen daraus den Schluss, dass die Dynamik des Cytoskeletts eine Schlüsselrolle für die Expression von Abwehr-Genen einnimmt, indem es zur Verstärkung der Transkription dieser Gene beiträgt.

1 Introduction

Both environmental and developmental signals play pivotal roles in the morphogenesis of the plants and for this reason, plants constantly sense their surroundings for clues to adjust their development. In contrast to their animal counterparts, plants lack sensory organs. Thus, the necessity to collect information about their surroundings imposes a severe challenge for the plants. However, this dilemma is efficiently overcome by conferring to each cell the ability for signal perception and transduction. However, this is of course not achieved without paying a price. Plants have to integrate the information reported by individual cells that is not only tremendous in quantity, but can also be contradictory with respect to quality. Thus, the morphogenesis of plants is controlled by a decision made on the whole plant level based on the information collected by individual cells according to the influences imposed by various external and internal stimuli.

Plants are static, but they are endowed with the capability of growth towards a beneficial environment (tropism). This kind of mobility is based on a polarity of cell division and expansion. During cell division, the microtubular preprophase bands (PPB) play a key role in defining division axis and symmetry. The position of a new cell plate after completion of chromosome segregation is determined by the position of the PPBs, which subsequently controls the pattern of branching. The second mechanism of adjusting tropistic growth is by cell expansion. However, the expansion axis is constrained by the orientation of microfibrils in the cellulosic cell walls, which is controlled by microtubules. Cortical microtubules guide cellulose synthesis and organize the orientation of microfibrils in parallel with MTs. Because cell growth and expansion is directional, plants can respond to environmental signals by growing in a direction positive or negative with respect to the environmental stimulus.

There is a growing evidence for the plant cytoskeleton as target for numerous signaling chains. The cytoskeleton has been found involved in sensing abiotic signals such as touch, gravity, mechanic stimuli, osmotic pressure, cold (for review see Nick, 2008a) and biotic signals (for review see Schmelzer, 2002). Signal sensing is generally subdivided into three main events: stimulus perception, generation and transmission of a signal, and subsequent changes in downstream biochemical processes (Yamaguchi , 2000). In this context it remains to be elucidated, whether the role of the cytoskeleton in abiotic sensing is limited to downstream processes or whether it can also act further upstream. Moreover, it is not clear, whether the role of cytoskeleton differs during sensing of biotic and abiotic stimuli.

1.1 Functions of cytoskeleton in plant cell morphogenesis

The plant cytoskeleton is a highly dynamic and versatile intracellular scaffold made up of microfilaments and microtubules which are composed of monomeric G-actin protein units and α -, β -tubulin heterodimer units respectively. The cytoskeleton plays a key role during plant cell growth and during developmental processes such as cell division, cell expansion, intracellular organization and vesicle trafficking. Control of cell morphogenesis by cytoskeleton can be achieved through the regulation of cell expansion, of cell wall structure and of cell division.

1.1.1 Roles of cytoskeleton in cell expansion and cell wall formation

Growth is a fundamental ability of all living creatures, and can either occur by increasing the volume of the existing cells or by increasing the numbers of cells.

Introduction

In plants, both mechanisms require the formation of new cell wall which is a rigid layer mainly composed of cellulose microfibrils arranged in parallel. Cell expansion is possible only when the constraint of cell wall is released through the hydrolysis of hydrogen bonds within the cellulose-hemicellulose network, the expansion occurs in a certain direction depending on the structure of this network. Due to co-alignment of microfibrils and microtubules, cortical microtubules are thought to control the direction of cellulose deposition and thus to determine the direction of cell expansion. The effect of microtubule drugs on cell growth supports this model. For instance, in roots of *Arabidopsis thaliana*, the microtubule inhibitors oryzalin and taxol stimulated radial swelling of the root apex (Baskin et al., 1994). Conversely, branched, anisotropically growing leaf trichome cells lost their capability for branching when treated with microtubule drugs (Mathur and Chua, 2000).

In coleoptile epidermal cells, microtubules are arranged in parallel bundles which are oriented perpendicular to the axis of potential cell expansion. A change of the axis of cell expansion is always found to be preceded by reorientation of cortical microtubule during coleoptile bending (Nick et al., 1990; for review see Nick, 2008b). Two models are proposed to explain the relationship between cortical microtubules and cellulose microfibril formation. In the “monorail” model, the cellulose synthesizing enzyme complexes move along the cortical microtubule filaments, therefore the orientation of the microfibrils is parallel to the microtubules (Heath, 1974). In the “guardrail” model (Herth, 1980), the movement of cellulose synthesizing enzyme complexes is constrained within the channels formed between cortical microtubules. However, there is still a debate, whether the spatial pattern of cortical microtubules are primarily responsible for controlling cellulose deposition, because there is also a feedback of the cell wall upon the organization of microtubules.

Tip growth, such as pollen tubes and root hairs, is accompanied by microfilament turn over and elongation (reviewed in Hepler et al., 2001). In this case,

Introduction

transvacuolar microfilaments are suggested to limit cell expansion by their rigidity. However, treated with the actin eliminating drug latrunculin B, cell elongation is inhibited rather than promoted (Baluška, 2001). This indicates that microfilaments do not play a key role in elongation, though they are involved in directional vesicle transport and positive growth regulation (reviewed in Nick, 2006).

With dual labeling strategies in living plant cells, Golgi vesicles and membrane-ensheathed organelles have been shown to move along microfilaments. When the microfilament network was disrupted by pharmacological agents, this movement ceased though the shape of the network was not altered radically (reviewed in Hawes and Satiat-Jeunemaitre, 2001). It is therefore conceivable that the disruption of the microfilament cytoskeleton will result in misdirected delivery of different vesicles to the cell cortex and thus cause expansion or division abnormalities.

1.1.2 Microtubule and cell division axis

The control of the cell axis in dividing cells is another key element of cell morphogenesis. When a plant cell prepares for mitosis, the nucleus, which is surrounded by microfilaments, migrates to the site where the prospective cell plate forms. At the same time, the radial microtubules which emanate from the nuclear envelope merge with the cortical cytoskeleton. Then the preprophase band (PPB) is laid down and marks out the site and orientation of the prospective cell plate. The guiding function of PPB is supported by experiments on mutants (Traas, 1995; McClinton and Sung, 1997). These mutants failed to form PPB and the ordered dividing pattern was replaced by a completely randomized pattern of cross cell walls. The division spindle is always laid down perpendicular to the PPB with the spindle equator located in the plane of the PPB. As soon as chromosomes move to the two poles, the microtubular

phragmoplast forms during late anaphase at the site that has been marked by the PPB.

1.2 Types of signal-triggered cytoskeletal responses

Environmental factors not only are used as guidance for the development of plants, but also very frequently challenge their survival. In addition to these abiotic stresses the plant has to cope with biotic stresses such as fungal attack. Increasing evidence shows that plant cells change the organization of cytoskeleton in space and time as a response to these stimuli. Preincubation with anticytoskeletal drugs will therefore impede or even stop the corresponding physiological response. For example, callose formation around the penetration site seems to be impaired after treatment with anticytoskeletal drugs (Kobayashi, 1997). Microtubules and microfilaments facilitate the migration of the nucleus towards the infective site rapidly after invasion by pathogen which is thought to support defence (reviewed in Schmelzer, 2002). The evidence indicates that the cytoskeleton is probably involved in both biotic stimuli sensing and signal transduction.

Microfilaments and microtubules can elongate or shorten by polymerization or depolymerization at both ends. Microtubules are polymers of α - and β -tubulin dimers. The tubulin dimers polymerize end to end into protofilaments. The protofilaments then bundle into hollow cylindrical polymers that elongate by addition of heterodimers at one (plus) end, whereas the opposite (minus) end will not elongate and often even loses dimers. Microfilaments are assembled from globular G-actin by polymerization at the barbed end and depolymerization at the opposite (pointed) end. The distinct directionality of cytoskeletal polymers in terms of growth and shrinkage will result in treadmilling of the monomers through the polymer. At steady-state, the polymerization rate matches the

depolymerization rate. Treadmilling confers to the cytoskeleton a flexible organization and thus facilitates the functional versatility of the cytoskeleton.

In plant cells, cytoskeletal arrays exist mostly in two forms, cortical and radial (transvacuolar) MFs/MTs. The cortical MTs/MFs are underneath the cell wall and usually arranged parallel to each other and in most cases perpendicular to the axis of preferential cell expansion, whereas radial MTs/MFs reach from the nucleus into the cell periphery and diffuse into a cortical array. Cytoskeletal reorganization is tightly associated with cell signaling mechanisms. Generally, the change can be categorized into four groups: reorientation, disorganization/disassembly, bundling, and post-translational modifications.

1.2.1 Reorientation

Arrays of cortical MTs or MFs in interphase often change their orientation in response to various stimuli. MT reorientation was found universally in relation to tropistic growth signals, such as gravity, light, and even mechanical force (Fischer and Schopfer, 1998). In coleoptiles and sunflower hypocotyls, the cortical MTs of the outer epidermis are aligned in parallel arrays with random angular distribution. Once changing the growth axis by gravitropic or phototropic stimuli, the MT reorientation is activated. The random pattern changes into a preferentially transverse pattern which is perpendicular to longitudinal axis. Similar phenomena can be triggered by exogenous IAA. Thus, it has been supposed to be used as a diagnostic test for an auxin-mediated growth response in terms of the Cholodny-Went hypothesis (Nick *et al.*, 1990). However, this kind of MT reorientation was also observed in mechanical bending (Fischer and Schopfer, 1998), therefore, the causal relationship between MT reorientations and growth responses is probably bidirectional.

Signals such as light, electrical fields, gravity and ion gradients have been found to affect the developmental pathway by asymmetric divisions (reviewed in Nick,

1999a). The cytoskeleton, especially the PPB, plays a key role in the determination of the cell division axis (see chapter 1.1.2). For instance, the asymmetric division of microspores can be inhibited by treatment with antimicrotubular drugs (Twell, 1998).

1.2.2 Disorganization/Disassembly

When plant cells are confronted with biotic or abiotic stress, this can result in MT disorganization or disassembly, for instance as a result of aluminum (Al) toxicity. In the tobacco cell line VBI-0, Al induced additional bundles of cortical microtubules (cMTs) in the first few hours, whereas the thickness of the individual bundles decreased as the exposure time prolongs (Schwarzerová, 2002). In maize roots, Al induced stabilization of cortical MTs in the elongation zone and a rapid depolymerization in transition zone (Horst, 1999).

MTs disassembly was found in response to low temperature. However, the degree of MTs disassembly is different depending on the cold sensitivity of respective plant. In chilling sensitive plants such as maize, tomato or cucumber, MTs disassemble at 0-4 °C, but only at 0 °C in moderately resistant plants such as spinach or beet. By cold hardening (i.e. pretreatment with chilling, but non-freezing temperatures) it is possible to increase microtubular resistance even to freezing temperatures (reviewed in Nick, 2000).

When coincubated with the plant defence elicitor cryptogein, a protein secreted by the protist *Phytophthora*, a rapid and severe disruption of microtubular network and transvacuolar MFs was induced in tobacco cells. Even after hyperstabilization with the MT depolymerization inhibitor taxol, the microtubular network was still disrupted. Interestingly, oligogalacturonides (OGs), a so called endo-elicitor derived from digested plant cell walls, which triggers a similar set of defence genes as cryptogein, does not cause these changes of MTs (Binet, 2001; Higaki, 2007) indicating that MTs respond selectively to

different biotic stimuli.

1.2.3 Bundling

Parallel to microtubular disorganization, cortical microfilament (cMFs) bundles were formed after treatment with the elicitor cryptogein, whereas the transvacuolar MFs were disrupted. These actin responses were followed by the initiation of programmed cell death (PCD) (Higaki *et al.*, 2007) suggesting that MFs bundling is involved in the regulation of PCD.

During the penetration of a fungus, MFs start to align towards the site of fungal appressorium and MF bundles increase between the site of infection and the nucleus. In many cases, shortly before or after penetration, the nucleus moves to the penetration site along these MF bundles (reviewed in Schmelzer, 2002). This MF based movement of the nucleus was also observed in root hairs (Ketelaar *et al.*, 2002).

MF bundling is used by cells to build the main long-distance tracks required for vesicle and organelle transport (Thomas *et al.*, 2009). However, during the delivery of vesicle cargo, MF bundling is an indicator for transport inhibition (reviewed in Nick, 2006). MFs respond through bundling and debundling to stimuli which trigger tropistic growth characterized by asymmetric cell expansion and cell division. Further investigation revealed that this process is regulated by the plant hormone auxin (Fig. 1.1; reviewed in Nick, 2010). These bundles detach into fine actin filaments in response to additional IAA or NAA, which facilitate auxin transport by promoting the recycling and/or localizing of the putative auxin efflux carrier PIN. Subsequently, debundled actin filaments will bundle again as a response to the reduced intracellular auxin concentration caused by auxin outflow generating an oscillatory feedback system consisting of actin and auxin (Fig. 1.1).

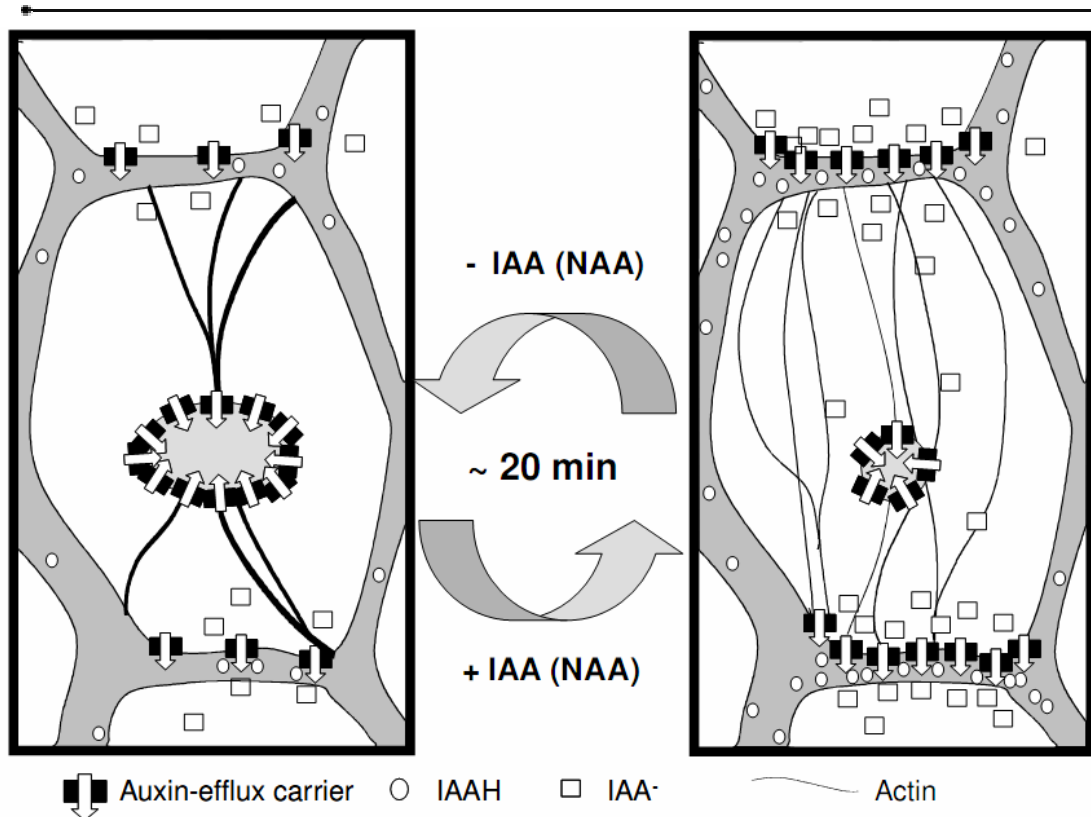


Figure 1.1 Model of the Actin-Auxin oscillator. MFs provide a track for auxin-efflux carriers, in the absence of auxin, MFs organize in bundles and auxin-efflux carriers cluster around the nucleus. These bundles detach into fine filaments in response to an increased auxin level before the commencement of auxin polar transport. (Cited from Nick, 2010).

1.2.4 Post-translational modifications

A subpopulation of α/β -tubulin heterodimers, the building block of MTs, undergoes post-translational modifications such as acetylation, glutamylation, phosphorylation and cyclic detyrosination/tyrosination (Hammond, 2008). For instance, all eukaryotic α -tubulins carry a conserved carboxyterminal tyrosine that can be cleaved and religated by specific enzymes, the detyrosinated tubulin dominates in stable microtubules, whereas microtubules with rapid turnover consist mainly of tyrosinylated tubulin. These modifications play an important role in regulating microtubule properties, as well as microtubule-based

Introduction

functions. However, their specific functional roles have remained mostly unknown so far.

Different tubulin isotypes have been described during signal induced microtubular reorientation (Duckett and Lloyd, 1994). In this study, stimulated cell elongation in dwarf pea stems coincided with a net shift of microtubule orientation from longitudinal and oblique to transverse and were accompanied by changes of the tubulin isotype, which can be distinguished by specific antibodies that can discriminate between tyrosinylated and detyrosinated α -tubulin (YL1/2 and YOL1/34, respectively). Detyrosination is not the cause of but rather the consequence of increased MT lifetime and length (Skoufias and Wilson, 1998). Wiesler (2002) show that signal-triggered microtubule re-orientation involves direction-dependent differences in tubulin tyrosination within single cells. This detyrosination/tyrosination alteration was detected by a couple of well-characterized monoclonal antibodies (Kilmartin, 1982; Kreis, 1987). The transversely oriented microtubules induced by auxin consisted predominantly of tyrosinylated α -tubulin, whereas the longitudinal microtubules induced by auxin depletion contained de-tyrosinylated α -tubulin. The authors suggested that longitudinal microtubules live longer as compared to transverse microtubules, which means that the stability of an individual microtubule would be indicated by its direction (Wiesler, 2002).

A recent study (Jovanovic, 2010) pointed out the importance of post-translational modifications of tubulin for the regulation of the cell cycle in plants. Irreversibly nitrotyrosinate α -tubulin which was produced by incorporation of nitrotyrosine (NO_2Tyr) instead of tyrosine into detyrosinated α -tubulin, can inhibit cell division by stimulation of cell elongation and misorientation of cross walls.

Actin depolymerizing factors (ADF) have been shown as stimulus-responsive modulators of microfilament dynamics including monomer binding,

Introduction

actin-filament binding/severing, and nucleotide/monomer dissociation-inhibiting. (Lappalainen , 1997; McGough and Chiu, 1999; Ouellet , 2001). In animal cells, actin cytoskeleton remodeling coupled with signal transduction is intermediated by actin-binding protein. MARCKS, a filamentous actin-crosslinking protein, is able to regulate actin-membrane interactions by integrating signals of protein kinase C and calcium/calmodulin (reviewed in Aderem, 1992).

Moreover, microfilaments can be stabilized by monoubiquitylation in response to pathogens and symbionts (Dantán-González , 2001). Contrary to polyubiquitylation chains at least four ubiquitin molecules for efficient recognition and degradation of targeted proteins, monoubiquitins often confer stability and different subcellular localization to proteins (reviewed in Hicke, 2001). The MFs in root nodules of were shown to be modified transiently by monoubiquitylation during nodule development. In addition, this response was found in root nodules of other legumes and other plants when infected with mycorrhiza or plant pathogens (Dantán-González , 2001).

1.3 The plant cytoskeleton in sensing of abiotic signals

1.3.1 Function of microtubules in response to abiotic stimuli

1.3.1.1 MTs in mechano- and gravity-sensing

An elegant experiment by Wymer 1996 indicated that MTs probably play a sensory role in mechano-sensing. Using agarose embedded tobacco protoplasts, cortical MTs and cell division planes were found to be aligned perpendicular to the force generated by centrifugation. They were able to show that this alignment could be disturbed by pretreatment with amiprophosmethyl (APM, a drug that

causes transient MT elimination) prior to centrifugation. Alignment of MTs and cell division planes remained unaltered in a control, where the protoplasts were treated with APM after centrifugation. A model to explain, how membrane deformations as consequence of mechanic stimulation can be transformed into biological input, assumes that the relatively stiff microtubules act as mechanical levers that convey force upon mechanosensitive ion channels (Fig. 1.2A).

MTs are also involved in gravity sensing as concluded from experiments, where gravitropic curvature, but not growth were affected after application of antimicrotubule drugs (Schwuchow, 1990). MTs reorientation was found to accompany gravitropic curvature and this reorientation was shown to be triggered by gravity directly, independently from mechanic stimuli caused by alterations of growth (Himmelspach and Nick, 2001). The classical theory for gravity sensing is based on the starch-statolith model. In this model, amyloplasts are used for the perception of a gravitropic stimulus. Further investigation revealed that the actual perception of gravity is not based on its translocation but on pressure imposed by statoliths on a small area (Hertel and Friedrich, 1973). Putting these two phenomena together, a function for MTs as amplifiers of the signal is emerging. Gravity can induce lateral transport of auxin and on the one hand this transport can be blocked by Ethyl-N-phenyl carbamate (EPC), a herbicide, which inhibits assembly of tubulin. On the other hand, taxol, which stabilizes MTs, inhibited lateral transport partially without any inhibition of longitudinal transport of auxin (Taylor and Leopold, 1992). These findings suggest that microtubular turn-over is involved in gravisensing (see Fig. 1.2 B).

1.3.1.2 MTs in cold sensing

As a transient, partial disassembly of MTs is sufficient to trigger cold hardening, plant MTs are proposed to be a thermometer (Abdrakhamanova, 2003). Intracellular calcium level increased rapidly in response to cold shock as detected using transgenic plants expressing the bioluminescent aequorin reporter (Knight

Introduction

, 1991). Further studies suggested that the dynamics of MTs is regulated via a calmodulin-sensitive interaction between MTs and MT-associated proteins (Durso and Cyr, 1994). Thus, a model according to which MTs have a dual function as primary sensor and signal amplifiers is proposed to explain these phenomena (Fig. 1.2 C).

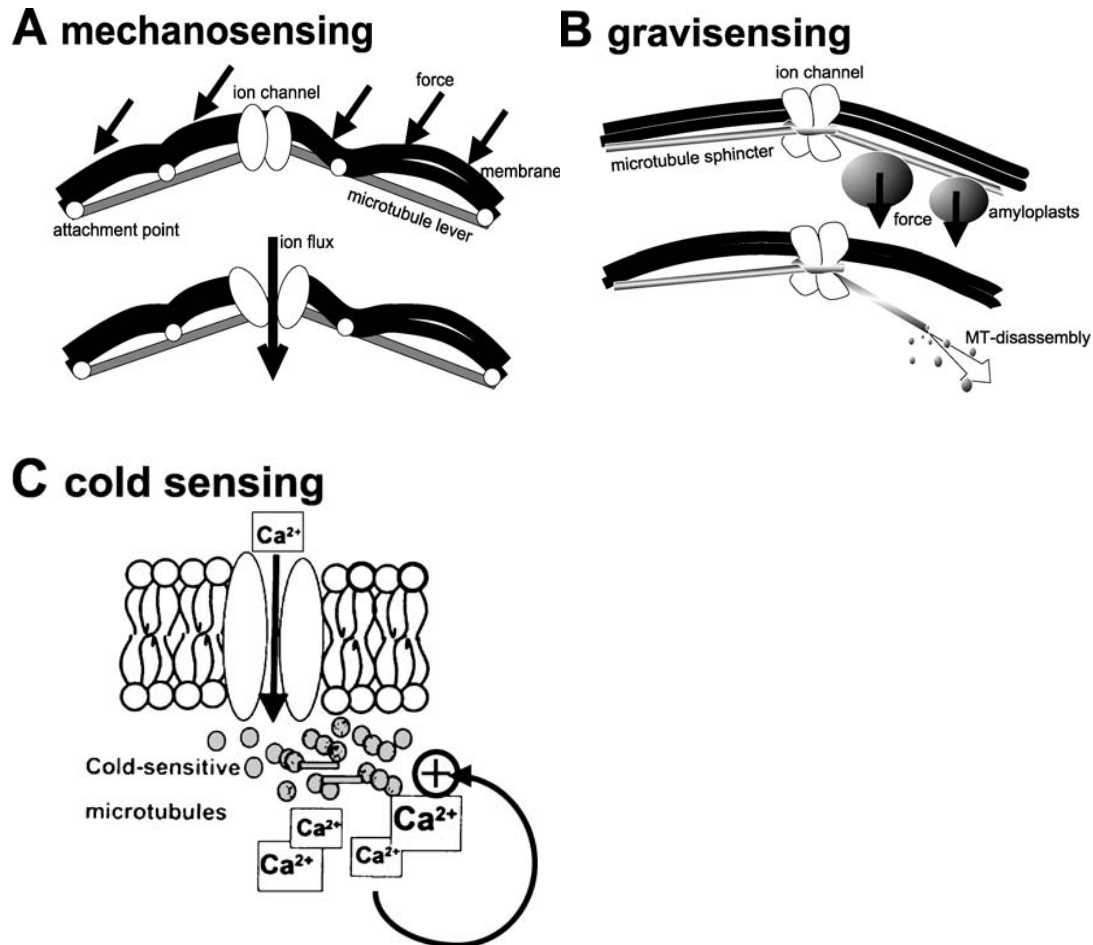


Figure 1.2 Function of MTs in touch, gravity and cold sensing. A. Mechanosensing: In this model, MTs attached beneath the membrane via some attachment point. To sense mechanical force, no dynamics of MTs are required. MTs and ion channels together serve as a stretch-active channel to gate the ion channel open and closure. Consequently, a physical stimulus is transformed into a chemical output. B. Gravisensing: In this model, MTs constrict the opening of ion channels and disassemble upon mechanic load. MTs form a special unit on the surface of an ion channel and the ion channel is closed accordingly. When mechanic force is loaded on the membrane, the MTs start to disassemble and the ion channel is released and become active. C. Cold sensing: In this

model, MTs control the permeability of mechanosensitive calcium channels. Cold can induce the cold sensitive MTs disassembly and amplify the influx of calcium. The calcium-triggered transduction cascade of gene expression will produce cold hardening. Then cold-stable MTs in consequence of cold hardening are formed. This indicates that post-translational modifications of MTs are involved in the signal transduction. Cited from Nick, 2008.

1.3.2 Functions of microfilaments in response to abiotic stimuli

MF reorientation is observed in response to several types of abiotic stimuli. MFs drive the motility and positioning of various organelles which is essential for the proper function of living cells, for example, translocation of chloroplasts under high light conditions (Kagawa , 2001). As MFs traverse statocytes, MFs were proposed to modulate amyloplast movement and also gravitropic signal transduction. Disruption of MTs by latrunculin B causes increased gravitropism in stem-like organs and roots which was speculated to be due to a more rapid settling of amyloplasts (e.g. Palmieri and Kiss, 2005 for roots).

MFs also participate in the protoplast volume control during the plasmolytic cycle (Komis , 2002). Although the mechanism of MFs in signal transduction is not well understood, there is growing evidence suggesting that this signal transduction pathway is mediated by ion channels. During the switch of stomata from open to closed, the MFs changed from well-organized cortical arrays to a disintegrated state (Eun and Lee, 1997). MFs involved in the regulation of guard cell volume were suggested to be modulators of the activity of ion channels in the plasma membrane (Hwang and Lee, 2001).

Interestingly, MFs were found to be able to respond very sensitively to electrical fields (Berghöfer , 2009). Nanosecond pulse electrical fields on tobacco cells caused a disintegration of the cytoskeleton at the nuclear envelope, accompanied by irreversible permeabilization of the plasma membrane. However,

when MFs were stabilized by phalloidin, which inhibits MFs disintegration, the perforation of plasma membrane was suppressed accordingly. Again, this indicated that MFs play a key role in signal triggered programmed cell death.

1.3.3 Actin, auxin, light and synchronized division patterns

To exploit the evolutionary advantages of multicellularity, the organism has to assign different functions to individual cells. In the framework of the open morphogenesis characteristic for plants, this cell differentiation is not achieved by a stereotypic cell-lineage, but by cell-to-cell communication (for instance, Van den Berg, 1995). Cormophytic land plants are constructed from modular elements, the telomes, which are differentiated from parenchymatic cells and organized around vasculature. The fossile record shows that the pattern of vascular differentiation already more than 375 million years ago was under the control of a polar flux of auxin (Rothwell and Lev-Yadun, 2005). In meristematic tissues of plants, the differentiation of newly added elements is determined by coordinative signaling from preceding elements, i.e., the pattern is perpetuated in an iterative manner (leaf primordia, Reinhardt, 2003; stem cells in the root, Van den Berg, 1995).

It was previously shown that suspension cell cultures of tobacco are endowed with a very simple form of pattern formation (Campanoni, 2003). The culture cycle in these lines usually originates from unicellular stages and proceeds through a series of axial cell divisions to produce cell files that are endowed with a clear axis and, in most cases, with a clear polarity (Campanoni, 2003). It has been found that cell division in these pluricellular files is partially synchronized, resulting in a higher frequency of cell files with even cell numbers over files with uneven cell numbers. This synchrony of cell division can be perturbed by NPA, an inhibitor of auxin transport (for review, see Morris, 2000).

Introduction

This suggests that division synchrony is under the control of polar auxin flux that coordinates the cell cycle of neighbouring cells (Nick, 2006).

In a tobacco cell line (*N. glauca* L. cv. Bright-Yellow 2), where actin was bundled as a consequence of overexpressing YFP-talin, the synchrony of cell division was impaired, but when the actin bundles were detached into finer strands by addition of IAA and, to a reduced extent, by NAA, the synchrony was restored (Maisch and Nick, 2007). These observations are consistent with published reports on actin-dependent transport of PIN proteins that are generally discussed as markers for auxin-efflux (for review see Muday and Murphy, 2002 or Blakeslee et al., 2005). However, this presumed link between actin organization and auxin transport has been recently questioned by experiments, where PIN1 and PIN2 maintained their polar localization, although actin filaments had been eliminated by the artificial auxin 2,4-dichlorophenoxy-acetic acid (2,4-D), or phytotropin naphthylphthalamic acid (NPA) (Rahman et al., 2007). Those contradictory phenomena pointed out that although actin seems to play a role for the polarity of auxin fluxes, the relationship is, first, not simple, and, second, far from being understood.

The molecular components that participate in the communication between actin and auxin remain mostly unknown. Generally, the nucleation of actin filaments is controlled by several, partially direct actin-associated, protein complexes including the Rho-related GTPases of plants (ROPs), the WAVE (for Wiskott-Aldrich syndrome protein family verproline homologous) complex, and the actin-related protein (ARP) 2/3 complex. These regulators modulate the actin cytoskeleton through an elaborate signaling network (for review, see Xu and Scheres, 2005). In fact, dual fluorescence visualization of actin and ARP3 in BY-2 cells demonstrated a graded distribution of ARP3 in the terminal cells of a file, and this gradient persisted when the file disintegrated into single cells, whereas the asymmetric distribution of the auxin-efflux marker PIN1 was lost and had to be re-established during the early phase of the new culture cycle (Maisch et al., 2007).

2009). These observations indicate that actin nucleation might be upstream of the events that culminate in a polar distribution of auxin efflux carriers.

1.4 The plant cytoskeleton in sensing of biotic signals

1.4.1 Cytoskeletal responses during host-pathogen interaction-How can a plant recognize and defend itself against pathogens?

Here are several barriers set for pathogen attack and the discrimination among them might not be very clear sometimes. A successful infection can be generally divided into six stages (Fig. 1.3) (Thordal-Christensen, 2003). Growing evidence shows that the cytoskeleton participates in the 3rd obstacle inducing barrier formation, such as papilla formation, callose deposition, protein and carbohydrate accumulation and even hypersensitive cell death.

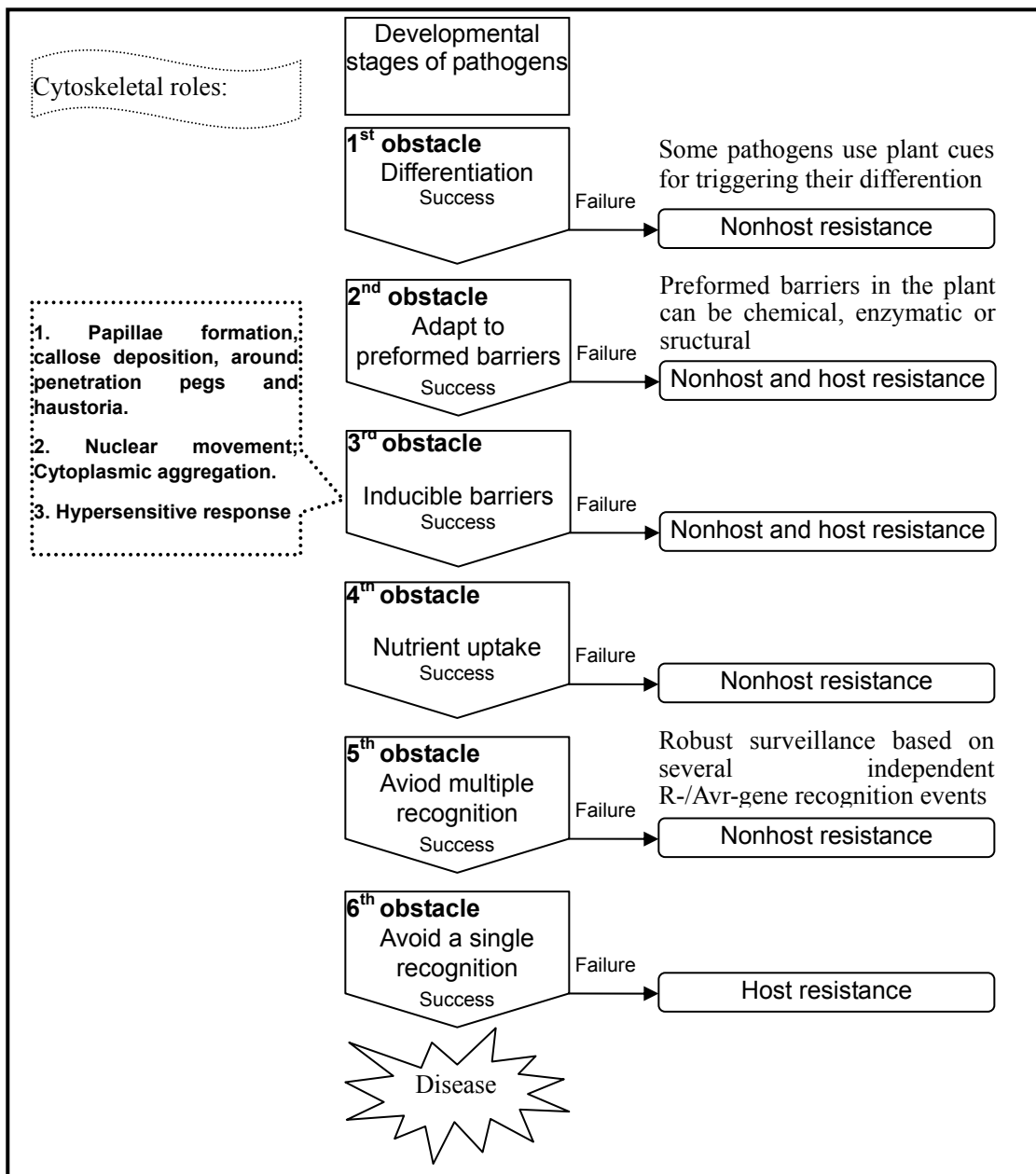


Figure 1.3 Infection stages and the involvement of host cytoskeleton in defence responses during pathogen attack. Modified from Thordal-Christensen, 2003.

Introduction

Once the pathogen attack is recognized by the host plant, a race is on. Beneath the fungal appressorium, the transversal cytoplasmic strands change their orientation towards this site and cytoplasmic streaming accelerates (Freytag, 1993). Already before penetration, the cytoskeleton was found to initiate reorganization, the MFs start to align towards the penetration site under the cell wall, and the MTs form radial arrays in the cortical cytoplasm (Fig. 1.4). Pharmacological experiments with anticytoskeletal drugs and reorientation of cytoskeletal components during the defence reaction suggest that the cytoskeleton plays a pivotal role for cellular defence. Pretreatment of barley coleoptiles with inhibitors of actin or tubulin polymerization or depolymerization before inoculating a non-pathogenic strain of *Blumeria graminis* has the consequence that the fungus was able to penetrate successfully and form haustoria in coleoptile cells of a non-host plant. Further investigations with different inhibitors show that actin filaments played a more active role than microtubules in penetration resistance (Kobayashi, 1997).

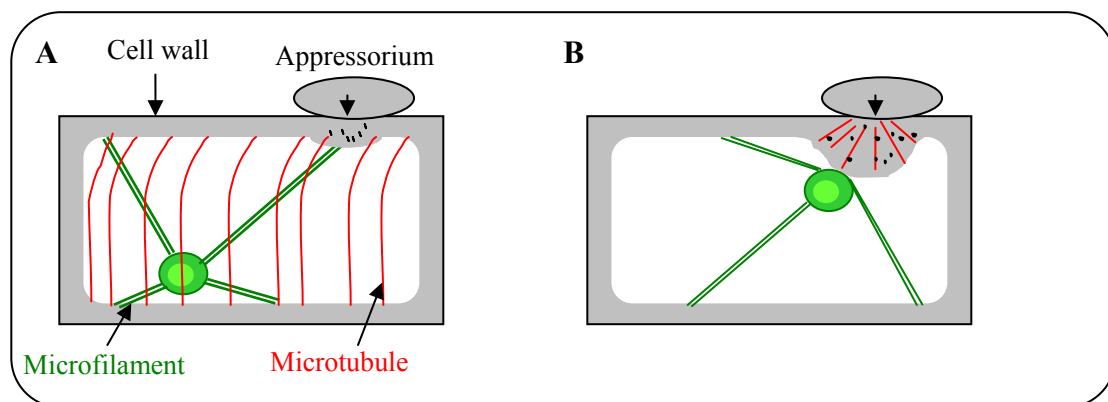


Figure 1.4 Cytoskeletal reorientation and papilla formation during pathogen penetration. A, Cortical microtubules are aligned in parallel lines and perpendicular to the longitudinal axis of the cell. However, transverse microfilaments form bundles and connect the nucleus and plasma membrane at the beginning of penetration. B, During penetration, the parallel cortical microtubules disappear and a radial array of microtubules assembles on the penetration site. The nucleus moves toward this site and massive local cell wall thickening starts heralding the formation of papilla. Modified from Schmelzer, 2002.

1.4.2 Elicitors triggered defence responses in plants

The interaction between pathogens and their hosts is subject to an evolutionary arm race, where the pathogens prevail by developing various strategies to circumvent or suppress defence responses of the host, whereas the host exceeds these responses through diverse approaches to identify and defend the invading pathogen. The so called gene-for-gene model has been established as the classical explanation for pathogen resistance and proposed that specific resistance genes (R genes) confer immunity to particular races of pathogens by the recognition of so called avirulence factors that are essential for the life cycle of the pathogen (for review see Dangl and Jones, 2001).

However, in recent years it became clear that the R-gene defence has to be seen as a highly specialized, derived situation that has evolved from much broader systems of defence that confer resistance to entire groups or classes of microorganisms. This nonhost resistance (for review see Heath, 2000; Thordal-Christensen, 2003) can be triggered by general elicitors, so-called pathogen-associated molecular patterns (PAMP, for review see Nürnberger and Brunner, 2002). In contrast to R-gene-dependent defence, the responses to general elicitors do not always result in programmed cell death. Typical examples for general elicitors are chitin (Felix, 1993) or bacterial flagellin (Felix, 1999; Zipfel, 2003). The signalling triggered by exogenous elicitors can be complemented by endogenous elicitors that are synthesized by the host-cell wall upon hydrolytic attack of pathogen-derived enzymes (Davis, 1984).

One of the cellular responses to elicitors is the formation of cell wall papillae around sites of pathogen penetration. The formation of these papillae is preceded by a reorganization of the cytoskeleton causing a redistribution of vesicles and a cytoplasmic aggregation towards the penetration site (for reviews see Takemoto and Hardham, 2004; Kobayashi and Kobayashi, 2008), and a slightly slower migration of the nucleus (for review see Schmelzer, 2002). By mechanical

Introduction

stimulation of parsley cells it was possible to partially mimic an attack by that are capable of inducing several aspects of a nonhost resistance including nuclear migration, cytoplasmic reorganization, formation of reactive oxygen species, and the induction of several defence-related genes (Gus-Mayer , 1998). In contrast, localized application of the corresponding elicitor (pep-13) failed to induce the morphological changes, although it induced the full-set of defence-related genes and the formation of reactive oxygen species. Interestingly, the elicitor treatment completely inhibited cytoplasmic aggregation and nuclear migration in response to the mechanic stimulus. Since pep-13 induces in this system the activity of a mechanosensitive calcium channel (Zimmermann , 1997), it seems that chemical and mechanical signalling converge during the cytoskeletal response to pathogen attack. Neither the mechanical stimulus, nor the elicitor, nor their combination was able to induce hypersensitive cell death in these experiments leading the conclusion that additional chemical signals are required to obtain the complete host pathogen response.

1.5 Dose cytoskeleton act upstream in signal transduction?

The cytoskeleton not only works as a static element like a scaffold or a barrier, but also actively responds to numerous signals by reorientation, bundling/debundling, and disassembly/assembly. These rapid, dynamic changes might qualify cytoskeleton as a candidate for signal perception, regulation, signal exchange but it might also just be a down-stream cellular response.

During cold acclimation in cold resistant wheat, cortical microtubules undergo transient disassembly while this response cannot be observed in cold sensitive cultivars. However, disassembly of microtubules mimicked by cytoskeletal drugs was able to induce cold acclimation in cold sensitive seedlings (Abdrakhamanova

, 2003). This suggested that cortical microtubule may act as gauges for cold acclimation. In addition, cortical microtubules are intimately associated with membrane which is a main platform for signal perception and transduction. The surface of cortical microtubules is covered with protein complexes, motor proteins and structural microtubule-associated proteins, GDP/GTP, regulatory kinases, phosphatases, and ions (reviewed in Wasteneys, 2003), which brings us a prospect of microtubules acting as repositories for signalling. In biotic stimulus sensing, inhibition of cytoskeletal dynamics can facilitate fungal penetration of host cell walls. These observations suggest that the cytoskeleton is actively involved in signal transduction. However, is the cytoskeleton just acting downstream in signal transduction, or does it also act upstream in sensing stimuli? In general there are two opposing opinions about it.

1.5.1 Cytoskeleton acts as a sensor or a regulator?

In this hypothesis, the cytoskeleton can receive, amplify and transduce signals. Therefore, it controls or partially controls the final biochemical or physiological output in response to various stimuli (Fig. 1.5 A). In other words, the way in which the cytoskeleton deals with signals resembles that of a perceptive mechanism (similar to a receptor). Consequently, once the function of the cytoskeleton is inhibited, the whole signaling chain (cascade) will be blocked and the corresponding biochemical or physiochemical output will be suppressed.

1.5.2 Cytoskeleton acts as a transducer?

The cytoskeleton might be just one step in a signal transduction chain, or even a target of cellular functions. This means that there are no direct causal relationship between cytoskeletal response and the cellular function triggered by the signal (Fig. 1.5 B).

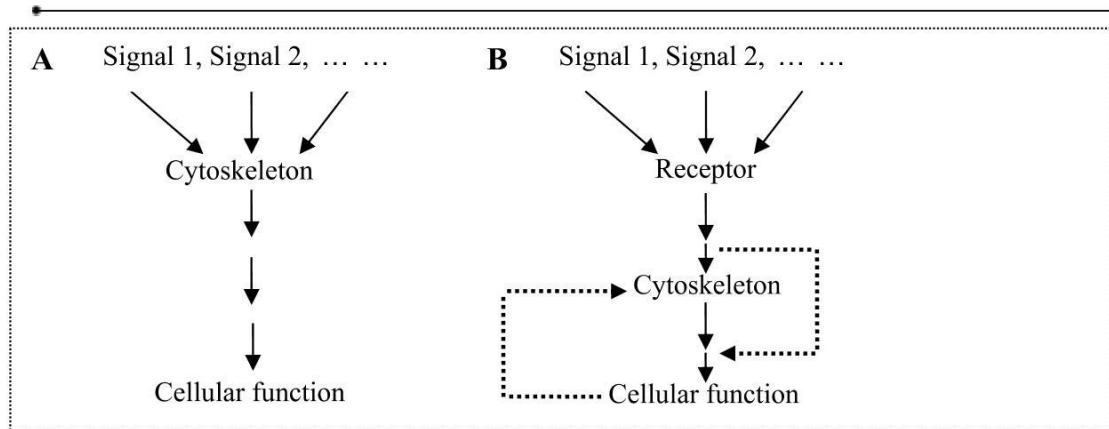


Fig. 1.5 Possible roles of the cytoskeleton in the response to signals. A, The cytoskeleton acts as perceiver/receptor. It can receive, transform, and transmit signals. B, The cytoskeleton only participates in signal transduction as a downstream-element.

1.6 Approaches of this study

1.6.1 Cytoskeletal responses to light in synchronized cell division pattern

The relationships between light triggered cell growth and the cytoskeleton are well documented (reviewed in Nick, 1999a). Cell morphogenesis can be controlled by cytoskeleton-dependent polar expansion or division. Considering the large amount of evidence supporting the role of cytoskeleton in signalling as well as the importance of light for plant growth and development, I presume that cytoskeleton might be a player in light sensing.

Due to the photosynthetic lifestyle of plants, the most relevant environmental signal for plant is light, it is used both as energy for photosynthesis and clue for development. The classical system to study light-dependent pattern formation has been the anthocyanin pattern in mustard cotyledons that is under control of the phytochrome photoreceptor system (Mohr, 1972). A cellular analysis of this patterning process revealed that the response of individual cells was very

Introduction

stochastic (Nick , 1993), with expression of a complete response in some cells coexisting with the complete absence of a response in even the neighbouring cells. These all-or-none-type differences even of adjacent cells were observed already for the early stages of the response (transcription of chalcone-synthase, a key enzyme for flavonoid synthesis). These responses are later coordinated and integrated throughout the entire organ. The patterns observed after microirradiation of different regions of the cotyledon could be explained by a working model, where the cellular responses were regulated by directional signals migration in apicopetal direction along the leaf veins.

However, the nature of these signals could not be revealed due to certain limitations of the experimental system. Mustard is very recalcitrant to transformation, and the very small cells of the young cotyledons are not amenable to cell-biological analysis. This stimulated the search for alternative systems to study pattern formation in plants. Tobacco suspension cultures with their patterned division response would be both accessible to genetic engineering and cell-biological analysis. However, they are not responsive to light, the most relevant environmental signal in plant life.

To overcome the drawback of the tobacco system, light responsive lines of tobacco have been searched. Success was achieved in isolating a derivative of the line VBI-0 that is responding to light (provided by Dr. Jan Petrášek). This line, VBI-3 has preserved the synchronized division patterning system of its progenitor line. These two properties in combination made it possible to investigate the interaction among synchronized division pattern, auxin, actin, and light in this tobacco cell line.

1.6.2 Role of cytoskeleton in response to the Harpin elicitor in grapevine

Traditionally, the role of the cytoskeleton has been seen as a response system that repartitions vesicle traffic and cytoplasmic architecture or executes pathogen-elicited programmed cell death. For instance, elicitor-induced reorganization of actin microfilaments was suggested to participate in the disintegration of the tonoplast during the hypersensitive response of tobacco BY-2 cells to the proteinaceous elicitor cryptogein (Higaki et al., 2007). However, a rising body of evidence (reviewed in Nick, 2008) suggests that cytoskeleton plays a role in the sensing of abiotic stimuli such as mechanic perturbation. This leads to the question, whether actin filaments and microtubules, in addition to their response to pathogens and elicitors, act upstream to elicitor-triggered signaling.

To address this question, a system was searched, where both cytoskeletal and defence responses could be triggered differentially by treatment with an elicitor. An experimental model was set up based on two cell lines from grapevine genotypes that differed in their sensitivity to the Harpin elicitor. cv 'Pinot Noir' is susceptible to pathogens such as *Botrytis cinerea* and *Plasmopara viticola*, whereas *Vitis rotundifolia* efficiently copes with infection by those pathogens (Jürges et al., 2009).

The Harpin elicitor has been isolated as a powerful so called type-III effector from *Bacterium*, the bacterium that causes fire blight of Rosaceae (Wei et al., 1992a). Since the *harpin* genes are conserved among phytopathogenic bacteria such as *Agrobacterium tumefaciens*, *Agrobacterium*, and *Agrobacterium* and were found to be essential for pathogenicity, they have been suggested to be the archetypical disease determinant of these pathogens. At the same time Harpin can trigger a hypersensitive response in non-host plants. The difference is ascribed to different

Introduction

ways of processing Harpin in host versus in non-host plants (Wei , 1992b). In addition to tissue collapse in tobacco leaves, Harpin triggers an alkalinization of the apoplastic pH. Due to its broadband efficacy as trigger of plant defence, Harpin was later commercialized under the brand name Messenger®.

As mentioned above, elicitors can mimic pathogens to trigger various defence responses; therefore, we used the Harpin response as model to dissect the role of the host plant cytoskeleton for plant defence in a single cell from a grapevine suspension cell line.

2 Materials and Methods

2.1 Cell lines

The tobacco (*Nicotiana glauca* L. cv. 'Virginia Bright Italia') cell line VBI-3 was selected as clonal line from the cell line VBI-0 (Opatrný and Opatrná, 1976) based on its ability to grow in the absence of exogenous auxin. Auxin-dependent VBI-0 cells were grown in slightly modified Heller's liquid medium (Heller, 1953) in the presence of the synthetic auxins 2,4-D (4.5 μM , Sigma-Aldrich, Deisenhofen, Germany) and NAA (5.4 μM , Sigma-Aldrich, Deisenhofen, Germany). To obtain auxin-autonomous lines, VBI-0 cells were selected in liquid medium without supplemental auxin over two successive subculture intervals until all files had completely disintegrated into individual cells. This suspension was then plated on solid auxin-free medium in petri dishes and cultivated in continuous darkness at 25°C. After 5 weeks small microcolonies were transferred to fresh auxin-free medium and cultured under continuous light. Cells were subcultured every 3 weeks, inoculating 3 ml of stationary cells into 30 ml fresh medium in 100 ml Erlenmeyer flasks.

Suspension cell cultures of *Vitis rotundifolia* and *Vitis vulpina* cv. 'Pinot Noir' generated from leaves were used as grapevine suspension cell culture lines. They were cultivated in liquid medium containing 4.3 g l⁻¹ Murashige and Skoog salts (Duchefa, Haarlem, The Netherlands), 30 g l⁻¹ sucrose, 200 mg l⁻¹ KH₂PO₄, 100 mg l⁻¹ inositol, 1 mg l⁻¹ thiamine, and 0.2 mg l⁻¹ 2,4-dichlorophenoxyacetic acid (2,4-D), pH 5.8. Cells were subcultured weekly, inoculating 8–10 ml of stationary cells into 30 ml of fresh medium in 100 ml Erlenmeyer flasks.

These cell suspensions were incubated at 25 °C in the dark on an orbital shaker

Materials and Methods

(KS250 basic, IKA Labortechnik, Staufen, Germany) at 150 rpm (18 mm diameter).

2.2 NPA and auxin treatments

Sterile-filtrated NPA was added at inoculation from a stock of 50 mM in DMSO to the final concentration of 5 μ M. For auxin treatment, either IAA (final concentration 2 μ M), or a combination of 2,4-D (final concentration 4.5 μ M) and NAA (final concentration 5,4 μ M) were added at inoculation after sterile filtration. Equal volumes of sterile DMSO and ethanol, respectively, were added to the control samples to account for possible effects of the solvent.

2.3 Quantification of pattern and morphology

From each sample, 0.5-ml aliquots of cells during the logarithmic culture phase were collected (days 7, 8, 9, 10 and 11 after inoculation) and immediately viewed under an Axiolmager Z.1 microscope (Zeiss, Jena; Germany). Frequency distributions over the number of cells per individual file were constructed from 200 individual cell files (containing up to ten cells per file) for each sampling day. The data from two independent experimental series with the five days in the two experimental series were pooled to construct frequency distributions over cell number per file, thus representing 2000 individual cell files. Cell densities were determined using a Fuchs-Rosenthal hemacytometer under bright-field illumination.

2.4 Light sources and irradiation

To assess the wavelength dependency of the light on patterning, the cells were cultivated in suspension at the conditions described above under continuous white light, red light (λ_{\max} 650 nm), far-red light (λ_{\max} 735 nm), and blue light (λ_{\max}

Materials and Methods

470 nm) adjusted to a fluence rate of $26.0 \mu\text{mol m}^{-2} \text{sec}^{-1}$.

The white light was obtained from cool white fluorescent bulbs (Atlanta Light Bulbs Inc., OSRAM L18W/25 UNIVERSAL WHI), blue light (AVAGO TECHNOLOGIES, HLMP-HB57-LP000), red light (VISHAY, TLDR5800) and far-red light (Quantum Devices, QDDH 73502) were obtained with LED arrays, respectively. The light intensities were measured by a quantum sensor (Skye Instrument Ltd., SKP 215) except far-red light which was measured by a custom-built photometer with a photodiode sensor.

2.5 pH measuring and recording

pH changes were monitored by pH meter (Schott handylab, pH12) connected with pH electrode (Mettler Toledo, LoT403-M8-S7/120) and recorded by a paperless record (MF Instruments GmbH, VR06) at intervals of 1 second. Before treatments, 2 ml of 3 or 4-day-old suspension cell were incubated on a shaker about 90 min till their pH values were stable.

To test the function of cytoskeleton drugs on Harpin inducible pH increase, cells were pretreated for 30 min with cytoskeleton drugs including phalloidin (1 μM), latrumculin B (1 μM), oryzalin (10 μM), taxol (10 μM) and cytocharasin D (5 μM). Solvents for different inhibitor were used as controls. After coincubation with these inhibitors, 9 $\mu\text{g/ml}$ Harpin were added to the suspension.

2.6 Microtubule visualization and quantitative analysis

Microtubules were visualized by indirect immunofluorescence using FITC (Eggenberger 2007). In brief, cells were fixed for 30 min with 3.7% (w/v) paraformaldehyde in microtubule stabilizing buffer (MSB: 50 mM PIPES, 2 mM EGTA, 2 mM MgSO_4 , 0.1% Triton X-100, pH 6.9) with self-made staining

Materials and Methods

chambers (Nick 2000), and then washed in PBS 3 times for 5 min. Subsequently, the cell wall was digested using 1% (w/v) Macerozym (Duchefa, Haarlem, The Netherlands) and 0.2% (w/v) Pectolyase (Fluka, Taufkirchen, Germany) in MSB for 5 min. Again, excess enzyme was washed out for 5 min with PBS. Unspecific binding sites were blocked for 30 min with 0.5% (w/v) BSA diluted in PBS. Directly after blocking, the cells were transferred into a 1:250 dilution of the primary antibody DM1A (Taufkirchen, Germany) in PBS for 1 hour at 37 °C in a moist chamber. To remove unbound primary antibody, the cells were washed 3 times for 5 min in PBS. Then the sample was incubated with a secondary FITC-conjugated antibody for 1h at 37 °C in a moist chamber. Unbound secondary antibody was removed by washing with PBS. Cells were then washed 3 times for 5 min in PBS and observed immediately by confocal laser scanning microscopy (TCS SP1; Leica, Bensheim, Germany) using the fixed-stage configuration of the confocal laser scanning microscope with the 488 nm laser line of the ArKr laser and a four-frame averaging protocol.

Microtubule's integrity was measured as described in Abdrakhamanova (2003). After transformation into binary images to eliminate differences in overall intensity, the images were filtered using the Find Edge algorithm. The result was an image where a profile across each microtubule yielded the same integrated density, irrespective of the thickness of the microtubule or its original fluorescence intensity. Under these conditions, it was possible to obtain a linear function between integrated density along a line intersecting the microtubule array, perpendicular to the orientation of individual microtubules and the number of microtubules intersected by this line. This function was used to calibrate the sample data. To obtain the sample data, a lattice of five equally spaced parallel lines, 8 pixels thick, was laid over each individual cell, so that the lines were oriented perpendicular to the microtubule array and did not touch the cell wall. The integrated density along each line was then determined with the Analyze algorithm, averaged for each cell and corrected for background measurements

Materials and Methods

obtained from the same image. Microtubule frequency (defined as the number of microtubules that are intersected by a line of 100 μm) was calculated from these density, by means of the calibration function.

2.7 Visualization of actin microfilaments

Actin microfilaments were visualized as described in Maisch and Nick (2007) with minor modifications.

For cells, suspension cells were fixed for 30 min in 1.8% (w/v) fresh paraformaldehyde in standard buffer (0.1 M PIPES, pH 7.0, supplemented with 5 mM MgCl_2 and 10 mM EGTA) containing 1% (v/v) glycerol and 0.1% (v/v) Triton X-100, cells were rinsed 3 times for 5 min with standard buffer.

For tobacco VBI-3 cells, suspension cells were fixed for 10 min in 1.8% (w/v) fresh paraformaldehyde in standard buffer (0.1 M PIPES, pH 7.0, supplemented with 5 mM MgCl_2 , and 10 mM EGTA) followed by a subsequent 10 min fixation in standard buffer containing 1% (v/v) glycerol. Rinse the cells with standard buffer twice for 10 min each.

Then, 0.5 ml of the resuspended cells were incubated for 30 min with 0.5 ml of 0.66 μM fluorescein isothiocyanate (FITC)-phalloidin (Sigma-Aldrich) prepared freshly from a 6.6 μM stock solution in 96% (w/v) ethanol by diluting (1:10, v/v) with phosphate-buffered saline (PBS; 0.15 M NaCl, 2.7 mM KCl, 1.2 mM KH_2PO_4 , and 6.5 mM Na_2HPO_4 , pH 7.2). Cells were then washed 3 times in PBS, 5 min each and observed immediately under confocal laser scanning microscopy (TCS SP1; Leica, Bensheim, Germany) using the fixed-stage configuration of the confocal laser scanning microscope with the 488 nm laser line of the ArKr laser and a four-frame averaging protocol.

2.8 RNA isolation and RT-PCR

1.5 ml of 5-day-old cells was induced with 9 µg/ml Harpin for 30 min, 2 h, 4 h, 6 h separately using water as control and harvested by low- speed centrifugation. Total RNA from *Arabidopsis thaliana* and *Nicotiana glauca* cv. “Piont Noir” cells was extracted using RNeasy Plant Mini Kit (Qiagen, Germany) and Spectrum™ Plant Total RNA Kit (Sigma, Germany) respectively, and then treated with DNA-free DNase set (Qiagen, Germany) to remove contaminating DNA. cDNA was synthesized from 1 µg of total RNA using M-MuLV RTase cDNA Synthesis Kit (TakaRa) according to the manufacturer’s instructions and the RNaseOUT™ Ribonuclease inhibitor (Recombinant) (Invitrogen, Germany) was used to remove the remaining RNA. PCR amplification was performed and the following PCR conditions were used: 30 cycles (94 °C, 30 s; 60 °C, 30 s; 72 °C, 1 min). Subsequently, the PCR products were examined by agarose gel electrophoresis. Levels of transcripts were quantified using Image J software relative to elongation factor 1a as internal standard. Results represent the fold increase of mRNA level over control cells referred as the uninduced control defined as 1x.

To test the function of cytoskeleton drugs on Harpin inducible gene transcripts, cells were pretreated for 30 min with cytoskeleton drugs including phalloidin (1 µM), patrumculin B (1 µM), oryzalin (10 µM), taxol (10 µM) and cytocharasin D (5 µM). 100% DMSO was used as solvent control and water as blank control. After pretreating, cells were induced with Harpin in indicated time points.

Materials and Methods

Table 1 Designations, sequences, and literature references for the oligonucleotide primers used to amplify the marker sequences used in this study. PR10 Pathogenesis-related proteins 10, respectively; PGIP polygalacturonase inhibiting protein; PAL1 phenylalanine ammonia lyase 1; CHS chalcone synthase; RS resveratrol synthase; StSy stilbene synthase; CHI chalcone isomerase.

Name	GenBank Accession	Primer Sequence 5'- 3'	Reference
EF1- α	EC959059	Sense: 5'gaactgggtgcttgatagc 3' Antisense: 5'aaccaaataatccggagtaaaga 3'	Reid, , 2006
PAL	X75967	Sense: 5'tgctgactggtgaaaaggtg 3' Antisense: 5'cgtccaagcactgagacaa3'	Belhadj , 2008
CHI	X75963	Sense: 5'gttcaggtcgagaacgtcc 3' Antisense: 5'gcttgccgatgatggactc 3'	Kortekamp, 2006
CHS	AB066274	Sense: 5'ggtgctccacagtgtgtctact 3' Antisense: 5'taccaacaagagaaggggaaaa 3'	Belhadj , 2008
PR10	AJ291705	Sense: 5'cttacgagagtgaggctcctc 3' Antisense: 5'gcaatagaacatcacaatactcc 3'	Kortekamp, 2006
PGIP	AF05093	Sense: 5'gatgtactgcgtcgaatg 3' Antisense: 5'gtggagcaccacacaagc 3'	Kortekamp, 2006
RS	AF274281	Sense: 5'gaaacgctcaacgtgcccaagg 3' Antisense:5'gtaaccataggaatgctatgtagc 3'	Kortekamp, 2006
StSy	X76892	Sense: 5'ggatcaatggcttcagtcgag 3' Antisense: 5'gtcaccataggaatgctatgc 3'	Kortekamp, 2006

2.9 Determination of cell viability

Aliquots (0.5 ml) from each sample were transferred into self-made staining chambers (Nick 2000) to remove the medium, then the cells were incubated in 2.5% (w/v) Evans Blue for 3 min, the Evans Blue were eliminated by washing with water twice. The frequency of the stained (unviable) cells was determined as well as the cell number per ml using a Fuchs-Rosenthal hematocytometer under bright-field illumination. The values reported are based on the observation of at least 1500 cells from three independent experiments.

2.10 Protein extraction and western blot analysis

Protein extraction was performed as described in Jovanović (2010) and Nick (1995), with minor modifications.

Protein extracts were prepared from 5-day-old grapevine cells 16 h after treatment with 9 μ M Harpin. After sedimentation in 15 ml falcon tubes (10min, 1500 g, Hettich Centrifuge Typ1300, Tuttlingen, Germany), Cells were homogenized in the same volume of precooled 0 °C extraction buffer, containing 25 mM MES, 5 mM EGTA, 5 mM MgCl₂, 1M glycerol, pH 6.9, supplemented with 1mM dithiothreitol (DTT) and 1mM phenylmethylsulphonyl fluoride (PMSF) by using a glass Potter on ice.

Insoluble tissue debris was removed by centrifugation (5 min at 13 000 g; Heraeus Instruments, Biofugepico, Osterode, Germany, Rotor PP1/96 #3324), followed by ultracentrifugation (15 min at 100 000 g, 4 °C; Beckman, USA, TL-100, rotor TLA100.2). Proteins in the supernatant were concentrated and precipitated with trichloroacetic acid. Then the sediment was washed with -20 °C 80 % acetone by vigorous vortexing. Again, the supernatant was discarded after centrifugation (30 min at 13 000g).

Samples were dissolved in 200 μ l sample buffer, incubated for 10 min at 95 °C, loaded onto a standard 10% SDS–mini gel, and subjected to western blotting as described in Nick (1995). A pre-stained broad range protein marker (P7708S, New England Biolabs) was used as a molecular weight standard. For detection of tyrosinated and detyrosinated α -tubulin, monoclonal antibody ATT (Sigma-Aldrich; Kreis, 1987) and DM1A (Sigma-Aldrich; Breitling and Little, 1986) were used at a dilution of 1:400 in TRIS-buffered saline containing TritonX-100 (TBST; 20 mM TRIS-HCl, 150 mM NaCl, 1% Triton, pH 7.4), respectively. Signal development was obtained by a goat secondary antimouse IgA, conjugated with

Materials and Methods

alkaline phosphatase (Sigma-Aldrich) at a dilution of 1:2500 in TBST with 3% low-fat milk powder. A parallel set of lanes loaded in exactly the same manner was visualized by Coomassie Brilliant Blue staining (CBB) to control the loading.

2.11 Quantification of growth response to oryzalin

The growth of the grape cell suspension culture was quantified by measuring the sediment volume of 15 ml suspension culture 7 d after subcultivation.

2.12 Programmed cell death detection

Programmed cell death was detected by in situ cell death detection kit, TMR red (Roche Diagnostics GmbH).

Preparation of sample material: 8-10 day old cells were incubated with 9 µg/ml Harpin for 24 h and then washed with PBS for 3 times. 100 µl of cells were inoculated with 100 µl of fixation solution (4% paraformaldehyde in PBS, pH 7.4, freshly prepared). Cells were resuspended and incubated at room temperature for 1 h, and centrifuged at 300 g for 10 min, subsequently, in order to remove fixative by sucking with tissue. Cells were washed once and supernatant was removed after centrifuge at 300 g for 10 min. Subsequently, cells were resuspended in 100 µl permeabilisation solution (0.1 % Triton X-100 in 0.1 % sodium citrate, freshly prepared) and incubate on ice for 2 min.

Labeling and microscopy: For positive control, cells were incubate with DNase 1 recombinant (3000 U/ml- 3U/ml in 50mM Tris-HCl, pH 7.5, 1mg.ml BSA) to induce DNA strand breaks. Cells were washed twice with PBS, then resuspend in 50 µl TUNEL reaction mixture and incubate at 37 °C for 1 h in dark. Wash twice with PBS and keep cells in PBS. For the negative control 50 µl lable solution were add. The nuclei were stained with

Materials and Methods

2'-(4-hydroxyphenyl)-5-(4-methyl-1-piperazinyl)-2,5'-bi(1H-benzimidazole) trihydrochloride (Hoechst 33258, Sigma-Aldrich) at final concentration of 1 µg/ml).

Cells were imaged under AxioImager Z.1 microscope (Zeiss) using the filter set DAPI (excitation at 365 nm, beamsplitter at 395 nm and emission at 445 nm) for all cell nuclei. Cells which have undergone programmed cell death were observed through the filter set HE (excitation at 550 nm, beamsplitter at 570 nm and emission at 605 nm).

3 Results

3.1 Light can rescue auxin-dependent synchrony of cell division in a tobacco cell line

3.1.1 Cell division pattern of VBI-3

The tobacco cell line cv. Virginia Bright Italia 3 (VBI-3) was derived from the tobacco cell line VBI-0 (Opatrný and Opatrná, 1976) as a clonal line selected for auxin autonomous growth in continuous light. VBI-0 and VBI-3 are similar with respect to their life cycle, cell file axiality and cell division synchrony (Fig. 3.1). The growth curves (Fig. 3.1A) plotted as cell density relative to the final cell density against time, are virtually identical for VBI-3 and VBI-0. As observed in the ancestral VBI-0, cell division in VBI-3 exhibits a clear axiality (Fig. 3.1B) and initiates from single cells and 2-cell-files (Fig. 3.1C) to generate pluricellular cell files. Frequency distributions constructed over the number of cells per file show higher frequencies of files with even cell numbers as compared to files with uneven cell numbers (Fig. 3.1D) as described for the ancestral line VBI-0 (Campanoni, 2003). However, in contrast to VBI-0, where cell division strictly requires exogenous NAA and 2,4-D (data not shown) cell division and synchrony are independent of NAA and 2,4-D. In contrast to the ancestral VBI-0, VBI-3 forms chlorophyll-containing plastids when cultured under light conditions as detected by chlorophyll autofluorescence (Fig. 3.1B). However, the synchrony of cell division is not significantly altered, when VBI-3 files cultivated in the dark are compared to those that were cultivated under white light (Fig. 3.1D).

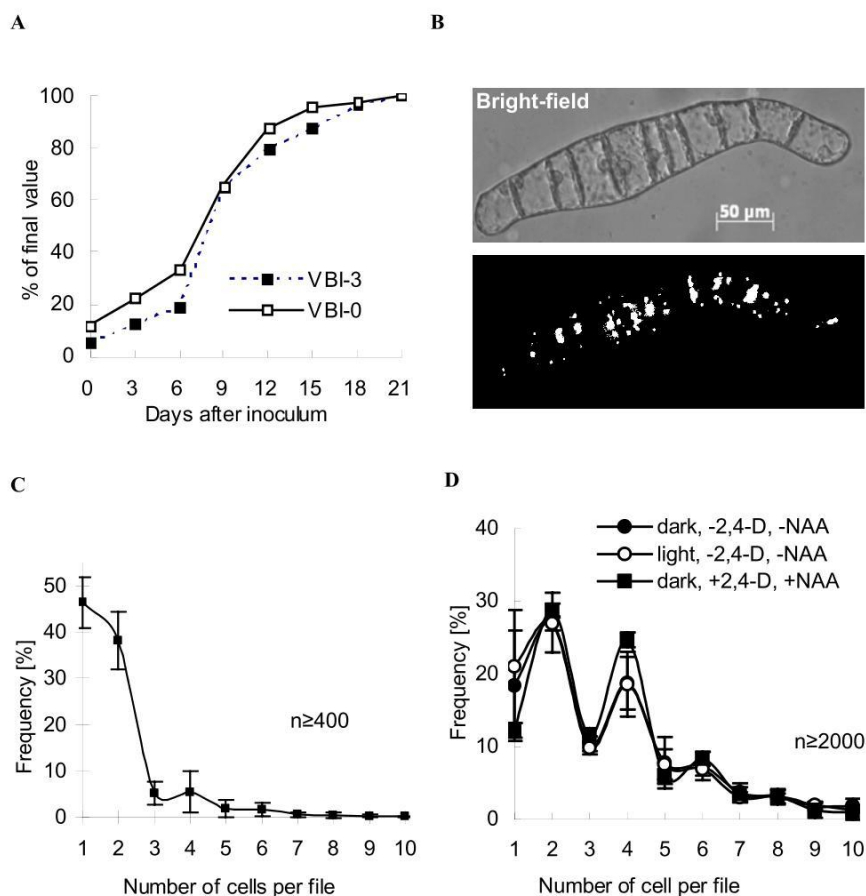


Figure 3.1 Cell division in VBI-3 follows a pattern that is independent of exogenous auxins. A, Cell density of VBI-3 and VBI-0 over time after subcultivation. Density is given relative to the final value after 21 days of cultivation. B, Morphology of VBI-3, bright-field and chlorophyll autofluorescence. C, Frequency distribution over number of cells per file at the initial state (day 0). D, Frequency distribution during the logarithmic phase in the presence of exogenous auxins (control) or the absence of NAA and 2,4-D for cultivation in the dark or under white light. The distributions are based on ≥ 400 (C) or ≥ 2000 (D) cell files from two independent experimental series. Error bars indicate SE.

3.1.2 The synchrony of cell division is affected by NPA and can be rescued by light or IAA

To investigate whether the division synchrony (monitored as predominance of even-numbered cell files) was dependent on auxin transport, NPA, an inhibitor of polar auxin transport, was added to the medium and cultivated in dark (Fig. 3.2A) or light conditions after subcultivation (Fig. 3.2B). Frequency distribution was altered in dark condition characterized by the decrease of the frequency of files with 4 and 6 cells (Fig. 3.2A), which eliminates the summit of files with 4 cells, i.e. the synchronization of cell division was affected. When the cells were cultured under white light, the peak of files with 4 cells was maintained in the presence of NPA, i.e. the impaired synchrony in response to NPA was rescued by light (Fig. 3.2B). To rule out the possibility that the rescue was mimicked by a photoinactivation of NPA, we performed a control experiment, where the medium complemented with NPA was irradiated under the same experimental light for 11 days and then used for subcultivation. This preirradiated medium caused the same perturbation of synchrony as medium freshly supplied with NPA (data not shown). Similar to white light, exogenous IAA could counteract the effect of NPA and restore the predominance of files with four cells over those with 3 or 5 cells (Fig. 3.2C). In combination with white light, exogenous IAA could eliminate the effect of NPA almost completely such that the division pattern of cultivated under a combination of white light, exogenous IAA, and NPA produced the same pattern as those cultivated in the absence of NPA (compare Figs. 3.2C and 3.2B).

Results

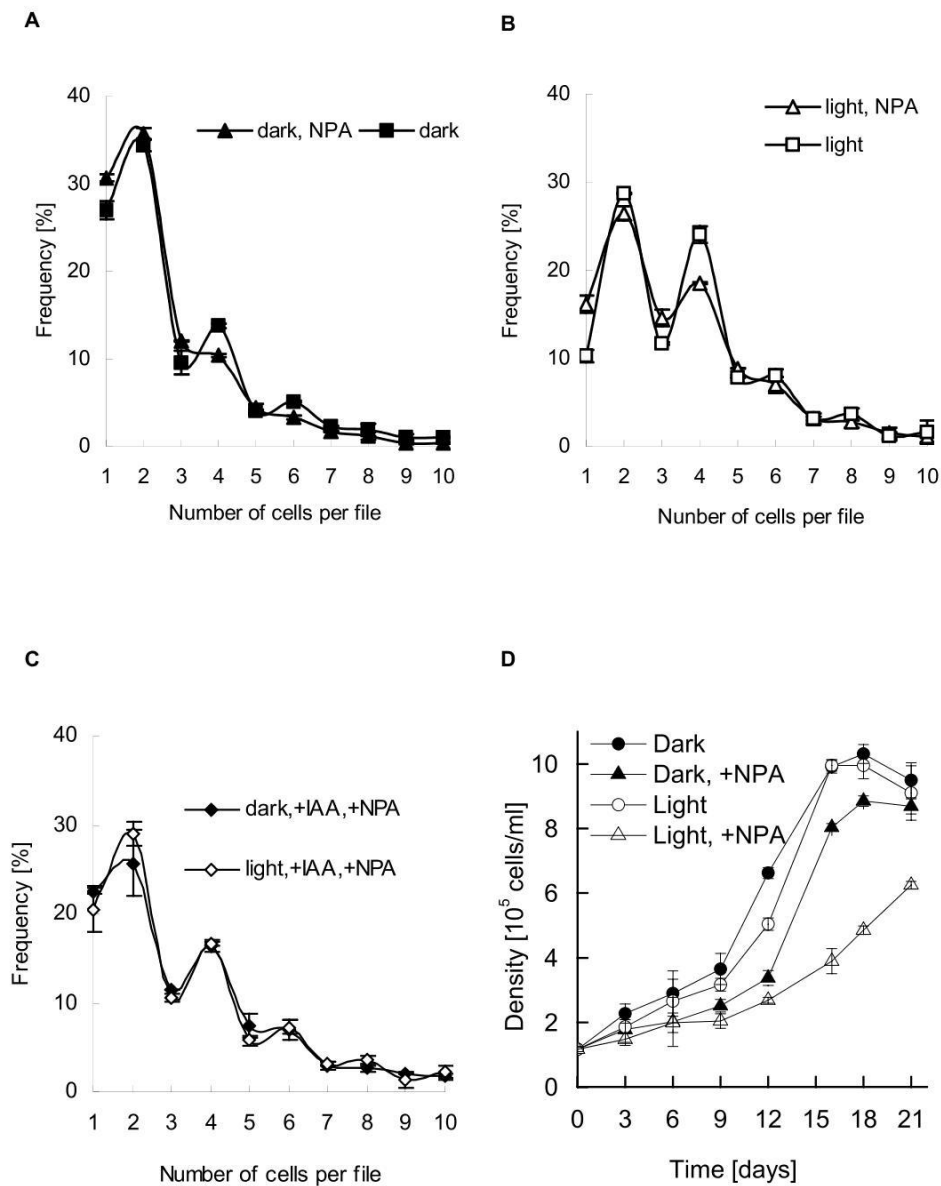


Figure 3.2 The effect of NPA on the division pattern can be rescued by light or exogenous IAA. Frequency distributions of cell number per file are shown for cells cultivated with 5 μM NPA, either in the dark (A), or under white light (B) or after treatment with 2 μM IAA (C). Control cells in A and B have been cultivated in the absence of NPA. Each distribution is based on ≥ 2000 cell files from two independent experimental series. D, Cell density over time after subcultivation in dark and light grown cultures in the absence or the presence of 5 μM NPA. Error bars indicate SE.

3.1.3 The rescue of the division synchrony by light depends on light quality

Since irradiation with white light counteracted the effect of NPA on the division synchrony, we are interested to test whether this reversal is light quality dependent (Fig. 3.3). For this purpose, cell cultures were kept in chambers irradiated with lights of different wavelenghtes. The results showed that continuous red light has a quite limited recovery ability (Fig. 3.3A). While cultures under continuous blue light present satisfactory recovery, especially files with less than 5 cells, regretfully the recovery is incomplete for longer files (Fig. 3.3B). Surprisingly, continuous far-red light can elevate the frequency of files with 4 and 6 cells (Fig. 3.3C) and the resulting frequency distribution became congruent with that observed in the absence of NPA (compare Figs. 3.3C and 3.2B). Thus, continuous far-red light can eliminate the disturbance of NPA on division synchrony.

Results

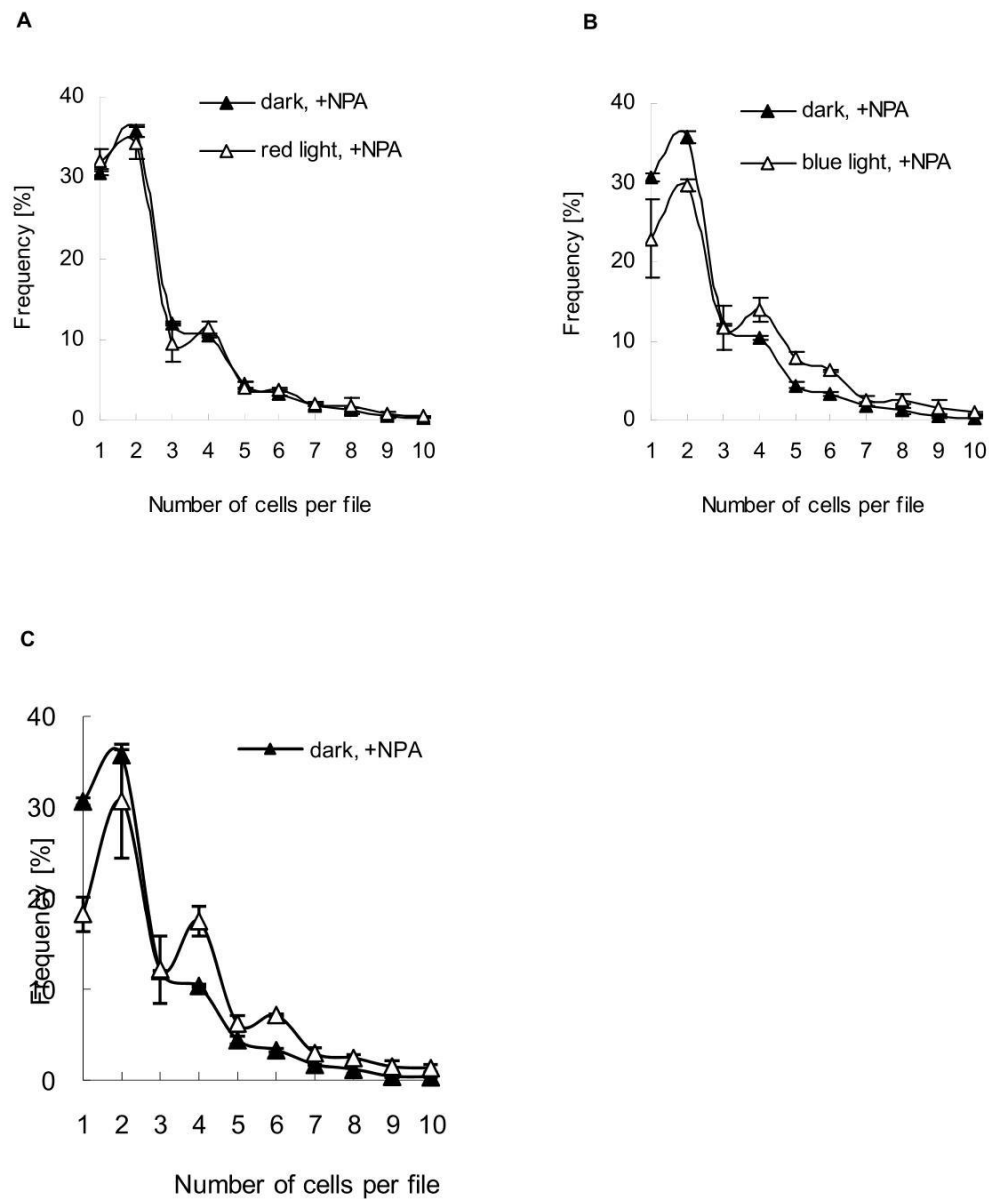


Figure 3.3 The light-dependent rescue of the division pattern in presence of NPA depends on light quality. Frequency distributions of cell number per file were constructed for incubation with 5 μM NPA under equal fluence rates ($26.0 \mu\text{mol}\cdot\text{m}^{-2}\cdot\text{sec}^{-1}$) of continuous red (A), blue (B), and far-red light (C). Each distribution is based on ≥ 2000 cell files from two independent experimental series. Error bars indicate SE.

3.1.4 NPA affects the organization of actin filaments

Division synchrony has been shown to depend on actin organization (Maisch and Nick, 2007), and the effect of certain phytohormones on auxin transport has been ascribed to the induction of actin bundles (Dhonukshe *et al.*, 2008), which put forward the question that how actin filaments respond to NPA in VBI-3. Actin filaments were visualized by fluorescent phalloidin in combination with a mild fixation protocol after 2 h, 16 h, and 24 h of incubation with 5 μ M NPA, respectively. The response of actin organization to NPA over time was followed by confocal microscopy. In the absence of NPA (but in presence of the solvent used for NPA, DMSO, in the same concentration as in the treated samples), transvacuolar actin strands reach out from the nucleus into the cell periphery and diffuse into a cortical actin array (Fig. 3.4A). 2 h after addition of NPA, this cortical actin array as well as the transvacuolar strands have significantly faded, whereas the perinuclear actin array has become more prominent (Fig. 3.4B). This repartitioning of actin towards the nucleus leads to a situation, where only a few bundles of actin emanate from the nucleus 16 h after addition of NPA (Fig. 3.4C) and eventually actin disintegrates into short fragments (Fig. 3.4D).

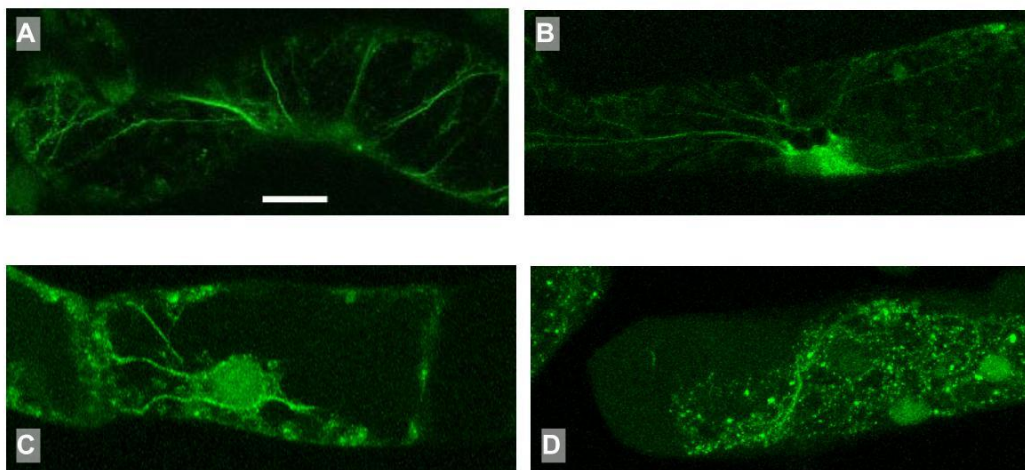


Figure 3.4 Effect of NPA on actin organization in VBI-3 cells after incubation for 2 h (B), 16 h (C), 24 h (D). The control (A) was treated with DMSO. 5 μ M NPA was added to the medium in the

presence of NAA and 2,4-D when subculturing. The cells were cultured in the dark. Projections from z-stacks through the entire cell are shown. Scale bar 20 μm .

3.1.5 Summary

Pattern formation in plants has to cope with ambient variability and therefore must integrate environmental cues such as light. Synchrony of cell divisions was observed in cell files of tobacco suspension cultures, which represents a simple case of pattern formation. The light response and auxin-autonomous cell line VBI-3 inherited this feature of pattern formation as its progenitor cell line VBI-0, cell divisions are synchronized during exponential growth phase.

Therefore, cell line VBI-3 should be an ideal candidate to assess the relationship among the division pattern and light and auxin. This synchrony can be inhibited by 1-N-naphthylphthalamic acid, an auxin transport inhibitor, and this process was accompanied by the disassembly of actin filaments. However, the synchrony can be rescued by white light or exogenous indolyl-3-acetic acid. The rescue was most efficient under continuous far-red light followed by continuous blue light, whereas the effect of continuous red light was quite limited.

3.2 Cytoskeleton acts upstream of the gene expression in response to the Harpin elicitor in grapevine

It is shown here that the two cell lines _____ and cv. 'Pinot Noir' differ with respect to the elicitor-response of microtubules and actin filaments. This is correlated with their different microtubule stability, and a differential response of defence-genes. Furthermore, the defence genes can be partially triggered by pharmacological manipulation of microtubules in the absence of elicitor providing

evidence for a role of the cytoskeleton acting upstream of elicitor-triggered gene expression.

3.2.1 Harpin induces extracellular alkalization

To monitor potential differences in response of the two cell lines to the Harpin elicitor, we used extracellular alkalization as indicator (Fig. 3.5). We observed in both cell lines that the pH increased rapidly and culminated about 30 min after addition of the elicitor and subsequently decreased. However, in cv. 'Pinot Noir', the peak of the response was delayed (after 2000 s) as compared to (after 1000 s). For cv. 'Pinot Noir', the response was accelerated and reached a higher amplitude, when the concentration of Harpin was increased from 9 µg/ml to 90 µg/ml (Fig.3.5C), however, in , there were no significant difference between the two concentrations (Fig.3.5D). To characterize the difference between the two cell lines on a quantitative level, time courses were recorded by varying the concentration of the elicitor. The results were fitted using a Michaelis-Menten equation with $pH_{max_{50}}$ (the time, when the pH response reached the half-maximum) as indicator of velocity. When $1/T_{pH50}$ was plotted over the concentration of Harpin (Fig.3.5E and F), saturable curves were found that fitted the Michaelis-Menten function well (R^2 0.805 for cv. 'Pinot Noir', and 0.600 for , respectively). From these functions, effective concentrations (EC_{25} , inducing 25 % of the maximal response) could be calculated to be 8.14 µg/ml for cv. 'Pinot Noir' and 1.65 µg/ml , respectively. This means that the affinity of is roughly five times higher as compared to cv. 'Pinot Noir'.

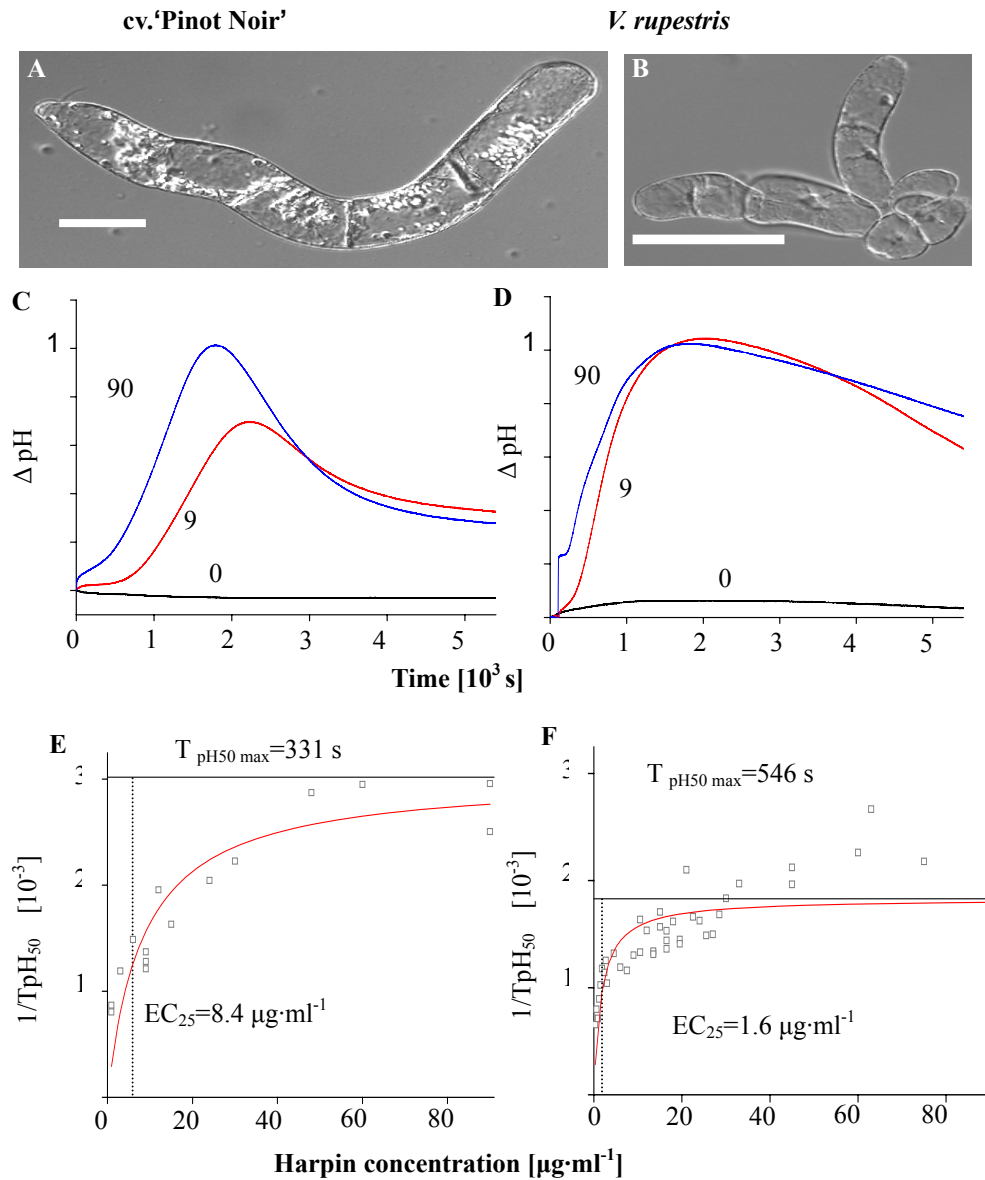


Figure 3.5 Cell morphology and response of pH to Harpin in cv. 'Pinot Noir' (A, C, E) and (B, D, F). A, B Cell morphology in differential interference contrast. Scale bar 50 μm . C, D Representative time courses of the pH response to 0, 9, and 90 $\mu\text{g/ml}$ Harpin. E, F Cumulative analysis of time courses in responses to increasing concentrations of Harpin. The data were fitted using a Michaelis-Menten function. TpH_{50} represents the time to reach 50% of the maximal response. The curves represent the average from $n = 15$ individual time courses.

Results

To investigate whether cytoskeleton dynamics are involved in Harpin triggered extracellular alkalinization, cytoskeleton disassembly or assembly inhibitors were pre-incubated with the cell culture for 30 min before Harpin was added. Both microtubule assembly inhibitor oryzalin and microfilament assembly inhibitors latrunculin B or cytochalasin D slightly decreased the pH response, while, the cytoskeleton disassembly inhibitor aggravated this response mildly. No difference between cv. 'Pinot Noir' and _____ was observed in this response.

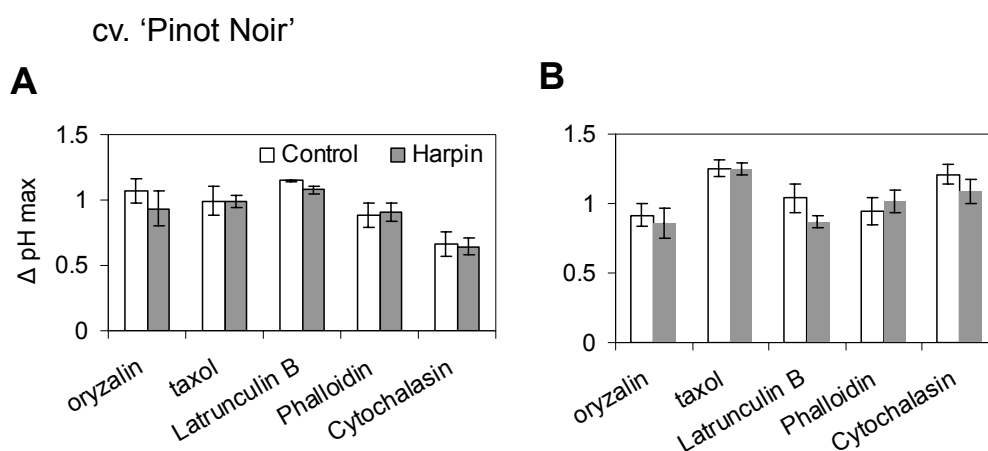


Figure 3.6 The effect of cytoskeleton drugs and Gd^{3+} on Harpin triggered extracellular alkalinization. Concentrations were 1 μ M for phalloidin, 1 μ M for latrunculin, 10 μ M for cytochalasin D, 10 μ M for oryzalin, 10 μ M for taxol. Controls of each treatment were incubated with solvent instead of inhibitor. Inhibitors and solvents were preincubated 30 min before Harpin were added to the suspension. Every value is the average of the maximum delta pH from 3 independent experiments. Error bars indicate SE.

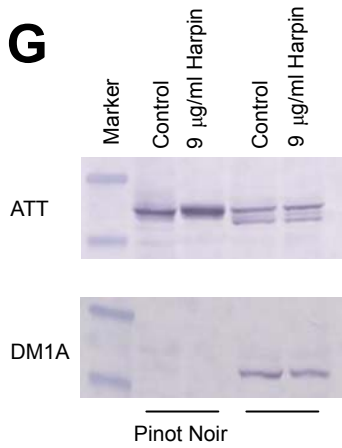
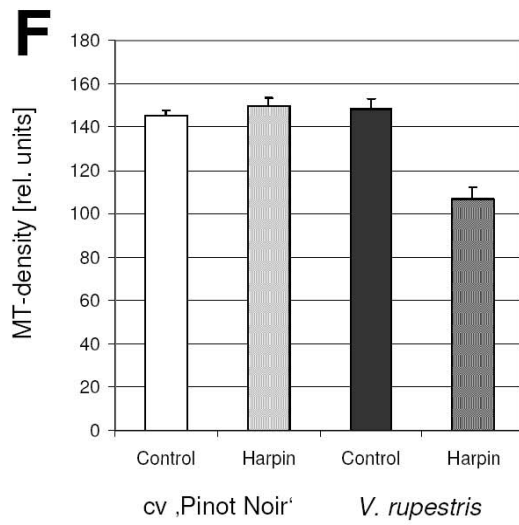
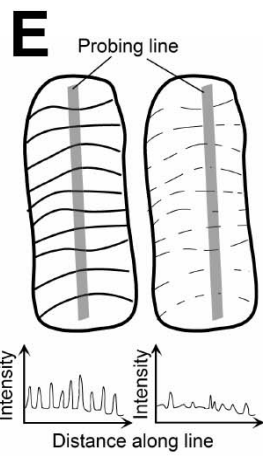
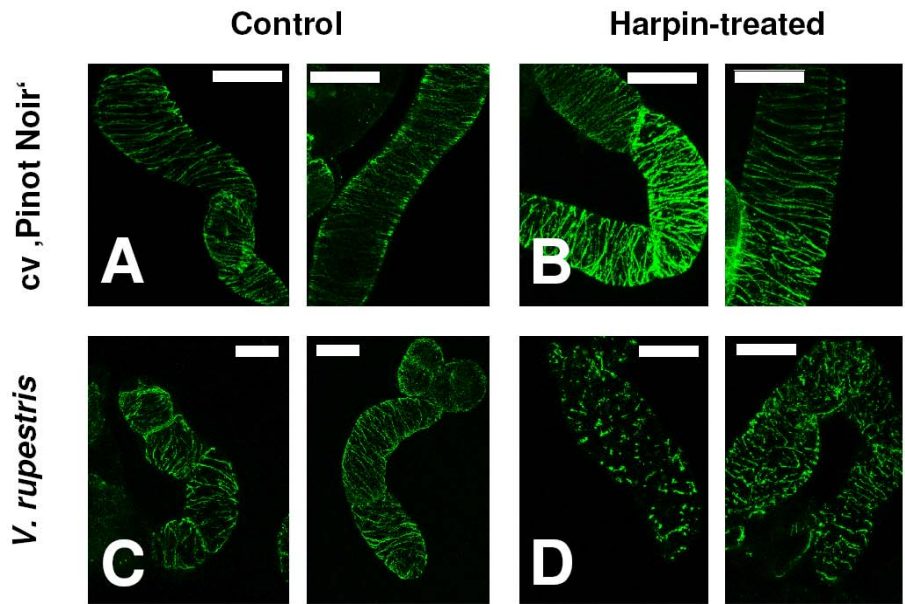
3.2.2 Harpin induces microtubule disintegration

Immunofluorescent staining combined with confocal microscopy are used to visualize the response of microtubules to Harpin. In control cells the microtubular network was organized in arrays of parallel bundles (Fig. 3.7A, C). In contrast, microtubules disintegrated after addition of 9 μ g/ml of Harpin (Fig. 3.7B, D). This response was more pronounced in _____ as compared to cv 'Pinot Noir'

Results

(Fig. 3.7D). This disintegration was perceptible already from 1 hour after addition of the elicitor (data not shown), and was completed at 3 hours (Fig. 3.7A-D). Since the degree of Harpin- induced microtubule disintegration varied between the two *Vitis* species, microtubule integrity was quantified as described in Abdрахманова (2003). As measure for integrity the number of microtubules intersecting a probing line perpendicular to the microtubule array was scored (Fig. 3.7E). Under control conditions, microtubule integrity was comparable between the two cell lines. However, in response to the elicitor, a differential behaviour became manifest. Microtubule integrity did not change significantly in the cv. 'Pinot Noir', although microtubules became finer after Harpin treatment (Fig. 3.7A, C). In contrast, in , microtubule frequency dropped dramatically (Fig. 3.7F).

To test whether the difference in the microtubular response is related to the difference in microtubular dynamic of this two species, the ratio between tyrosinylated and detyrosinated α -tubulin, as an indicator for the dynamic of microtubule, was assessed by Western blotting (Fig. 3.7G). Detyrosination is stimulated with increasing lifetime of microtubules and therefore can be used to monitor global microtubule turnover. The relative abundance of tyrosinylated α -tubulin (recorded by the ATT antibody) versus detyrosinated α -tubulin (recorded by the DM1A antibody) was generally elevated in cv. 'Pinot Noir' over and even increased slightly in response to the elicitor. In contrast, detyrosinated tubulin, which was hardly detectable in cv. 'Pinot Noir', was constitutively elevated in . This indicates that microtubules in cv. 'Pinot Noir' are generally endowed with higher turnover as compared to .



Results

Figure 3.7 Response of cortical microtubules to Harpin in cv. 'Pinot Noir' (A, B) and (C, D). Representative geometrical projections from z-stacks collected prior to (A, C) or 3 hours after (B, D) treating with 9 $\mu\text{g}/\text{ml}$ Harpin. Microtubules were visualized by immunofluorescence. Scale bar 50 μm . E, Method to quantify microtubule density (as a measure of microtubule integrity) as integrated fluorescence along a probing line. F, Microtubule density in relative units prior to (open bars) or after 3 hours of treatment with 9 $\mu\text{g}/\text{ml}$ Harpin (striped bars). Error bars represent standard errors. The values summarize the data of 18-39 individual cells collected from at least three independent experiments. G, Relative abundance of tyrosinylated α -tubulin (recorded by the ATT antibody) versus detyrosinated α -tubulin (recorded by the DM1A antibody) in total extracts from cv. 'Pinot Noir' or that had been either raised under control conditions or challenged for 24 hours with 9 $\mu\text{g}/\text{ml}$ of Harpin. The same amount of total protein was loaded to each lane.

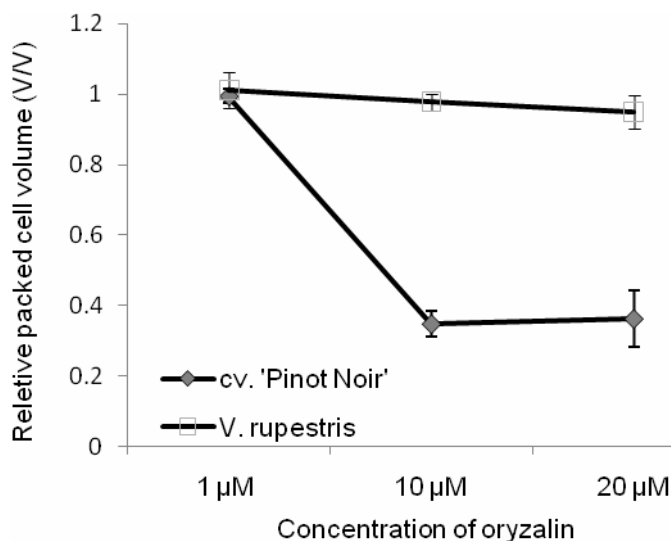


Figure 3.8 The effect of oryzalin on cell growth. 1 μM , 10 μM and 20 μM oryzalin was added at subcultivation. After 7 d, the packed cell volume was measured and plotted relative to unchallenged control cells. Error bar represent SE.

To verify whether the MTs consisted by detyrosinated tubulin is more stable than tyrosinated one and this stability is important to maintain their physiological functions, the effect of oryzalin on cell growth was investigated. Oryzalin, a microtubular assembly inhibitor, cause the microtubular network disassembly,

consequently, the cell growth is inhibited, which can be read out by the method of packed cell volume for suspension cell culture (Jovanović 2010). When 10 μ M oryzalin was added at subcultivation, the cell growth was significantly inhibited in cv. 'Pinot Noir', however, it only has a slight suppression on (Fig. 3.8) which the microtubular network is composed by a higher percent of deetyrosinated tubulin.

3.2.3 Harpin induces actin bundling

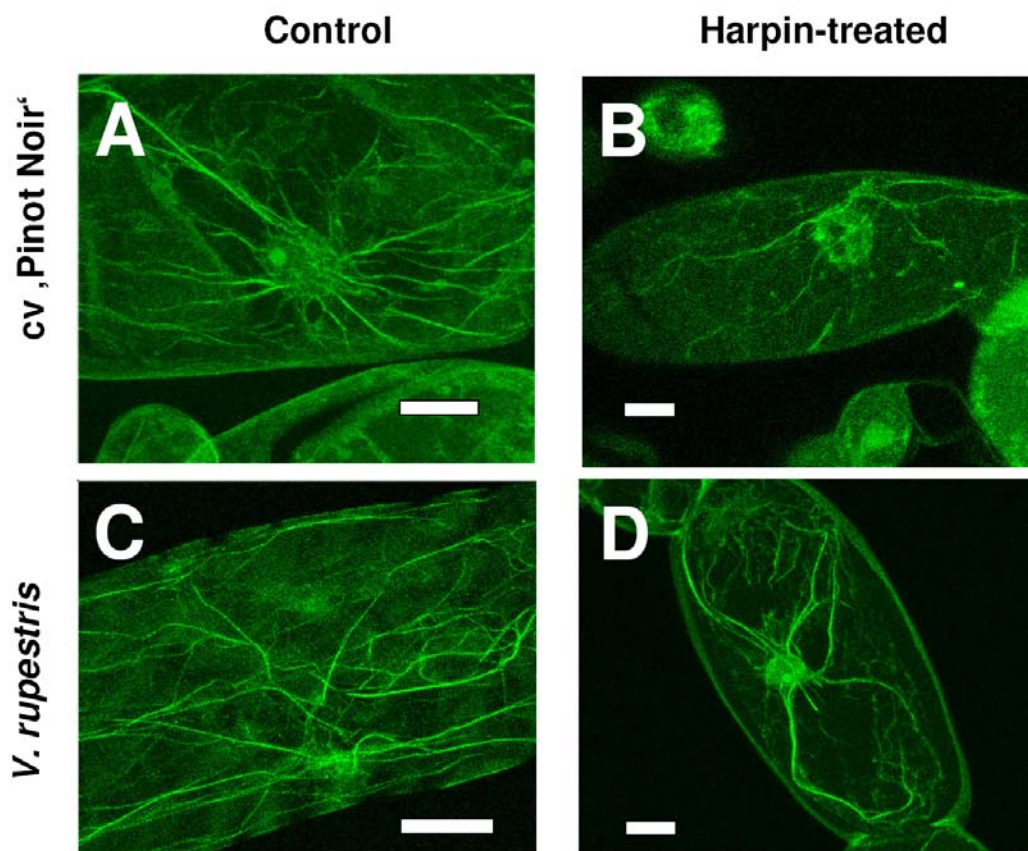


Figure 3.9 Response of actin filaments to Harpin in cv. 'Pinot Noir' (A, B) and (C, D). Representative geometrical projections from z-stacks collected prior to (A, C) or after 3 hours (B, D) of treatment with 9 μ g/ml Harpin. Actin filaments were visualized by fluorescence-labelled phalloidin. Scale bar 20 μ m.

Results

Since the resistance of plant cells to penetration by a pathogen has been shown to depend on actin organization (Kobayashi *et al.*, 1997; for review see Schmelzer, 2002), the response of actin filaments to Harpin was assessed in the two cell lines. Actin filaments were visualized by fluorescent phalloidin in combination with mild fixation after 3 h incubation with 9 μ g/ml Harpin. In the absence of Harpin, transvacuolar actin filaments reach out from the nucleus into the cell periphery and spread into a cortical actin array in both cell lines (Figs. 3.9A and C). In contrast, 3 h after addition of Harpin, the cortical actin array had faded obviously, and the finer transvacuolar actin filaments had been replaced by bundles that converge to the nucleus (Figs. 3.9B and D).

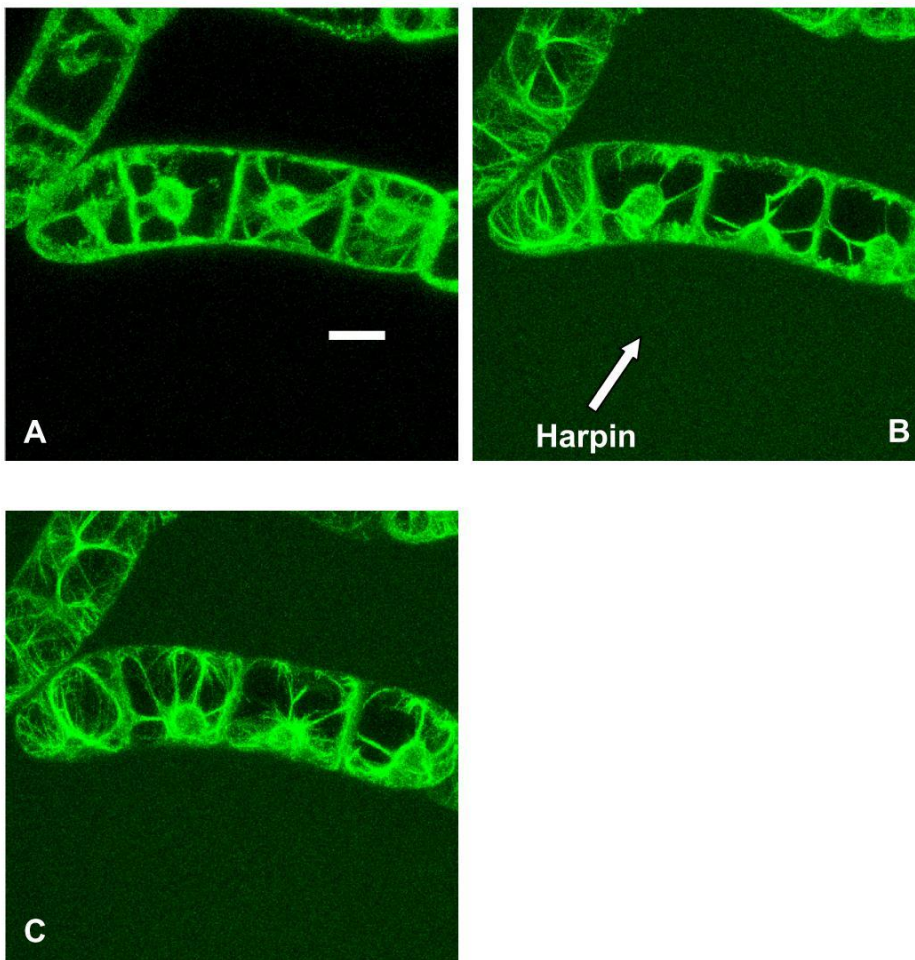


Figure 3.10 Polarity application of Harpin on microfilaments organization and nucleus movement in a transformed tobacco cell line BY-GF11, which stably expresses a GFP–fimbrin ABD2 fusion protein. Before the Harpin was applied (A), the microfilaments bundling was much less abundant than after a drop of Harpin was added at the down-left corner of the cover slide (B and C).

In most cases, the nucleus moves along the microfilaments bundles to the penetration site during pathogen invasion (for review see Schmelzer, 2002). To test whether the elicitor Harpin, as a mimicking pathogen, is able to trigger this phenomenon, microfilaments and nuclei were observed *in vivo* in a transformed cell line BY-GF11. In this cell line, microfilaments bundles formed directly after Harpin was applied, and the nuclei moved from the cell center towards the side where Harpin was added (Fig. 3.10 B and C).

3.2.4 Harpin induces defence-related genes

To estimate expression of defence-related genes in the two cell lines, suspension cells were challenged with 9 µg/ml of Harpin, and mRNA was isolated at different time points after induction (0, 0.5, 2, 4, and 6 h). The transcripts of all genes expressed were reversely transcribed into cDNA, which was used as a template for PCR analysis. Defence-related candidate genes were amplified by PCR, and their expression levels were normalized using elongation factor 1 α gene as internal reference. Genes involved in the phenylpropanoid pathway, such as phenylalanine ammonia lyase (PAL), chalcone synthase (CHS), chalcone isomerase (CHI), stilbene synthase (STS), and resveratrol synthase (RS) were used (Fig. 3.11), and complemented by the pathogenesis-related protein PR10, and the polygalacturonase inhibiting protein PGIP encoding the polygalacturonase inhibiting protein. Transcripts corresponding to genes RS, StSy, and PAL accumulated transiently in both cell lines.

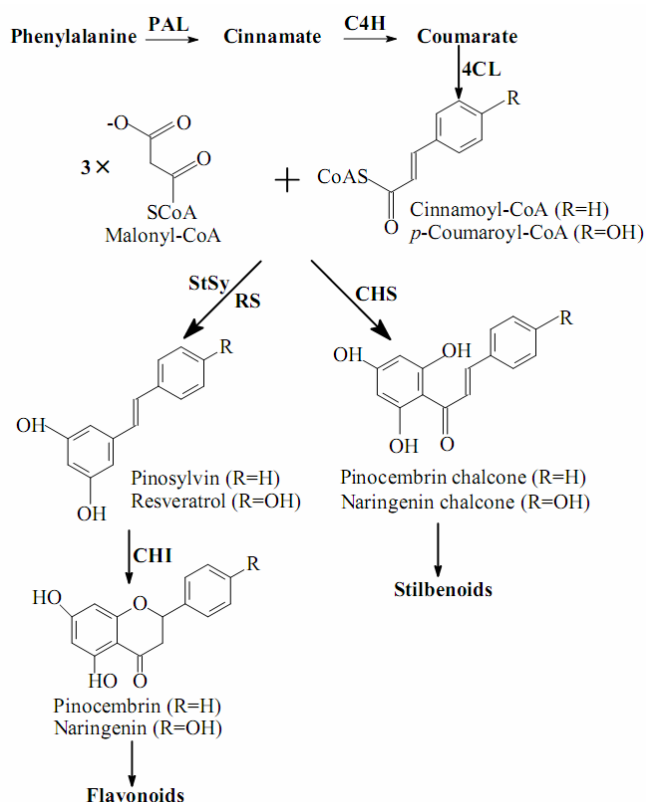


Figure 3.11 Position of the analyzed enzymes in flavonoid and stilbene metabolism.

However, the response initiated earlier and reached a higher amplitude in _____ as compared to cv. 'Pinot Noir'. CHS and CHI were constitutively upregulated in _____ as compared to cv 'Pinot Noir'. The expression of PR10 and PGIP was inversely regulated with respect to the phenylpropane enzymes with a stronger and earlier induction in cv. 'Pinot Noir' as compared to _____. Interestingly, the expression of StSy and RS that catalyze the same biochemical reaction during the biosynthesis of resveratrol, differs quantitatively, with a much stronger response of StSy gene (about fivefold as compared to RS). Nevertheless, for both genes, the response was much more pronounced in _____ over cv. 'Pinot Noir' (Fig. 3.12).

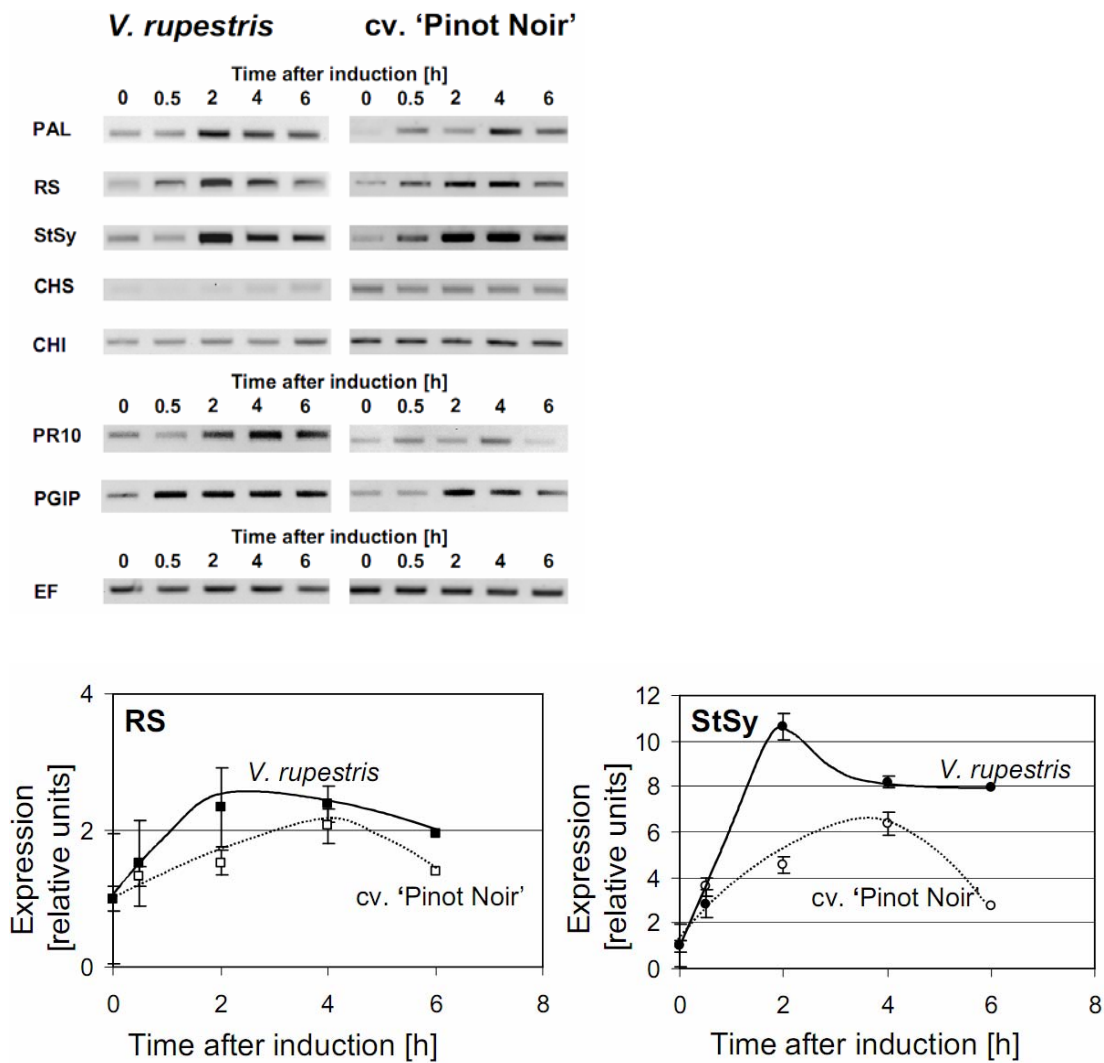


Figure 3.12 Response of defence-related genes to Harpin in cv. 'Pinot Noir' and *V. rupestris*. A Representative time courses of transcript abundance followed by RT-PCR in response to $\mu\text{g/ml}$ Harpin. The upper group represents genes of the flavonoid and stilbene pathway with PAL phenylalanine ammonium lyase, CHS chalcone synthase, StSy stilbene synthase, RS resveratrol synthase, and CHI chalcone isomerase, the middle group represents pathogenesis related genes with PR10 pathogenesis-related protein 10, and PGIP polygalacturonase inhibiting protein, elongation factor 1 α (EF) was used as internal standard for quantification. B Time course of transcript abundance for resveratrol synthase (RS), and stilbene synthase (StSy) relative to elongation factor factor 1 α . Data represent averages from three independent experimental series. Error bars represent standard errors.

3.2.5 Cytoskeletal compounds induce RS and StSy in the absence of elicitor

To gain an insight to the potential role of cytoskeleton of plant cells in response to elicitors, expression of the defence genes triggered by Harpin are compared with the target genes expression pattern induced by manipulation of the cytoskeleton. Both cell lines were incubated for 30 min either with drugs targeted to actin filaments (phalloidin, latrunculin B, cytochalasin D) or to microtubules (oryzalin, taxol) (Fig. 3.12). After 30 min, in one set of samples, 9 µg/ml of Harpin were added and gene expression assayed 2 hours later at the maximum of the response, whereas in the other set of samples, cells were not challenged by the elicitor. In the elicitor-treated set, the expression of RS and StSy was not significantly different between the drug-treated samples showing that the compounds did not impair the ability of the cells to respond to the elicitor.

Interestingly, there was a partial (up to a third of the maximal response), but clear induction of RS and StSy in the absence of the elicitor. Similar to the previous experiments, the induction was generally more pronounced in *C. rosaceus* as compared to cv 'Pinot Noir', and more prominent for StSy as compared to RS. Independent of these differences, a consistent pattern emerged with the strongest induction reached by oryzalin. Taxol produced a similar, but somewhat weaker induction, indicating that it is not the mere presence of microtubules, but in addition their turnover that negatively regulates the expression of these defence genes. Pharmacological manipulation of actin yielded weaker effects that were barely significant – if at all there was a tendency for induction in *C. rosaceus* by latrunculin B, a drug that eliminates actin filaments very efficiently.

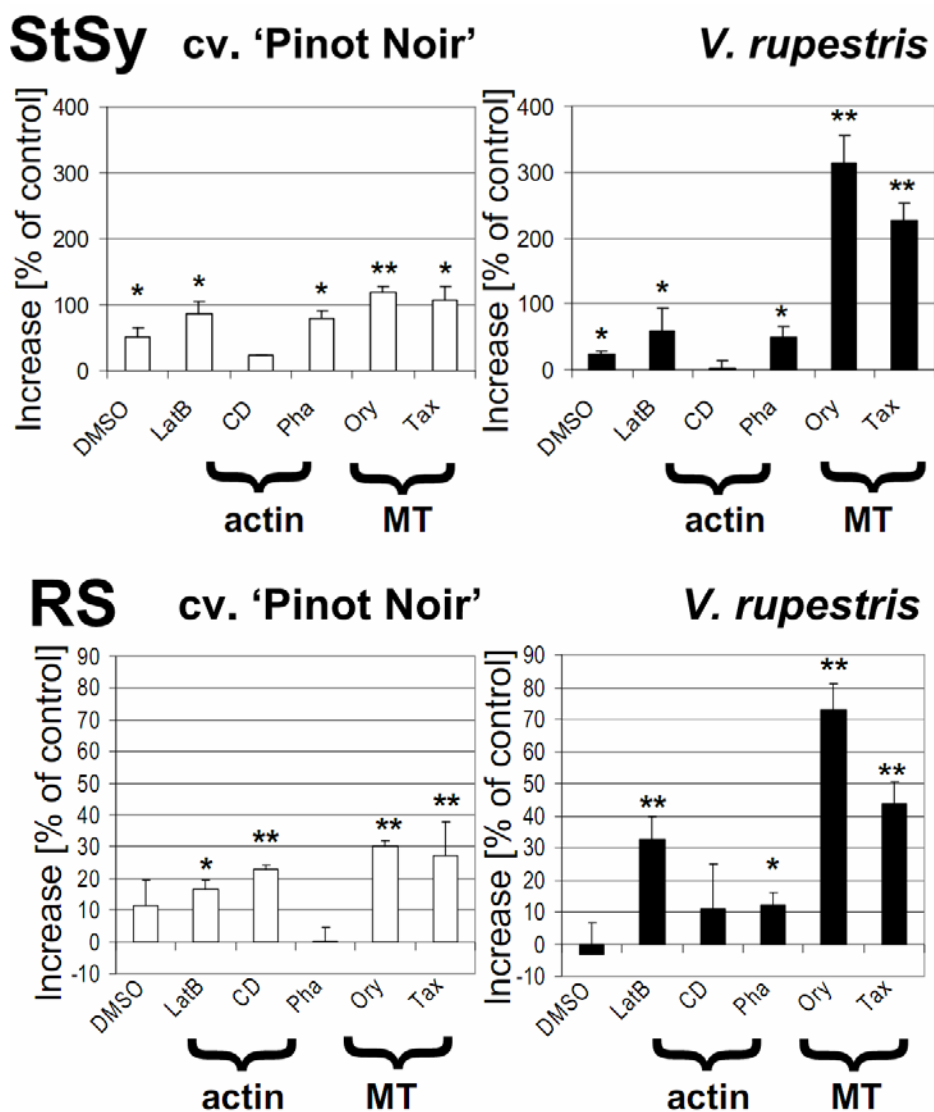
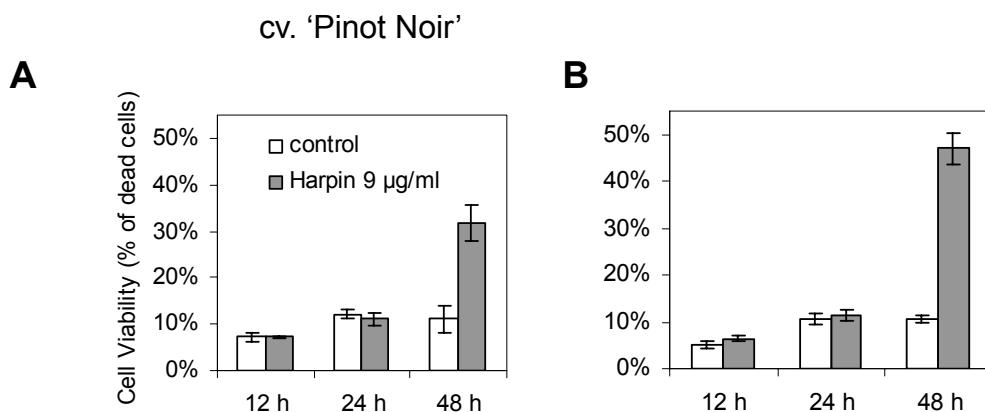


Figure 3.12 Expression of resveratrol synthase (RS), and stilbene synthase (StSy) relative to untreated controls after pretreatment with anticytoskeletal compounds for 30 min and allowing the response to be expressed for 2 additional hours. Concentrations were 1 μ M for phalloidin (Pha), 1 μ M for latrunculin B (LatB), 10 μ M for cytochalasin D (CytD), 10 μ M for oryzalin (Ory), 10 μ M for taxol (Tax), and 1 % for DMSO as solvent control for the oryzalin experiment. Data represent averages from three independent experimental series, error bars represent standard errors. * difference with untreated control significant at the 95 % confidence level, ** difference with untreated control significant at the 99 % confidence level.

3.2.6 The effect of Harpin on induction of cell death

Harpin can induce cell death in cv. 'Pinot Noir' and . After 24 h coincubation with Harpin, mortality of cell increased promptly, it reached a higher level in than in cv. 'Pinot Noir'. Was programmed cell death (PCD) triggered by Harpin? A rapid PCD can restrict multiplication and spread of pathogen at the site of infection, and it can also facilitate the uninfected part of plant to get systemic acquired resistance (SAR). Therefore, the rate of PCD in the cell line were tested and the results (Fig. 3.13 C and D) shown that PCD were partially induced. However, there was no significant difference between them.

Harpin can induce generation of ROS (Desikan et al., 1998). The accumulation of ROS can trigger on both necrosis and PCD. When ROS is overaccumulation, it acts as phytoalexin, therefore, necrosis occurred. When it is not enough to kill the cell directly, a signaling cascade can be switched on which will lead to PCD (reviewed in Van Breusegem and Dat, 2006). Hence, we conclude that Harpin initiated different level of cell necrosis in these two cell line might be the results of different amount of phytoalexin production.



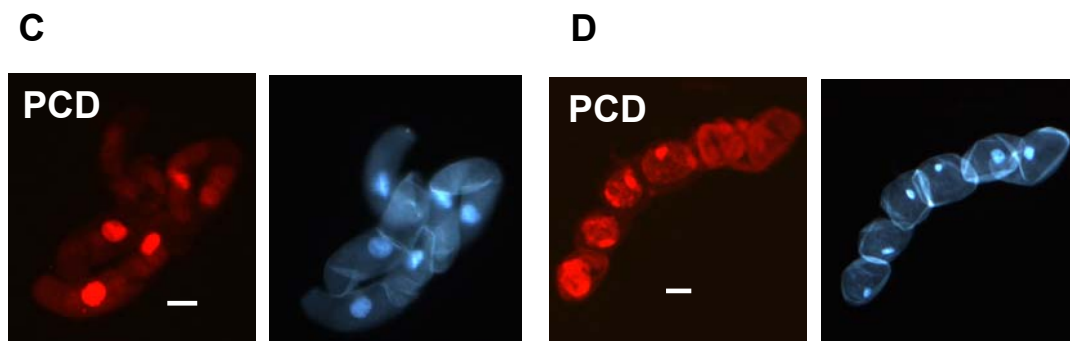


Figure 3.13 Cell viability was estimated by the percent of dead cell after Evans blue staining (A and B). Harpin was directly added in during subculture. In both cv. 'Pinot Noir' (C) and (D), cell underwent programmed cell death as assayed by TMR red kit after coincubation with Harpin for 24 h. Bar 20 μm .

3.2.7 Summary

Cytoskeleton undergoes dramatic reorganization during plant defence. This response is generally interpreted as part of the cellular repolarization establishing physical barriers against the invading pathogen. To get insight into the functional significance of cytoskeletal responses for defence, we used two cell cultures that differed in their microtubular dynamics and followed the cytoskeletal response to the elicitor Harpin in parallel to alkalization of the medium as fast response, and the activation of defence-related genes.

In one cell line derived from the grapevine cultivar 'Pinot Noir', microtubules contained mostly tyrosinylated α -tubulin indicating high microtubular turnover, whereas in a cell line derived from the wild grapevine, the α -tubulin was strongly detyrosinated indicating low microtubular turnover. The cortical microtubules were disrupted and actin filaments were bundled in both cell lines, but the responses were more prominent in as compared to cv. 'Pinot Noir'. Cytoskeletal responsiveness correlated with elicitor-induced alkalization and the expression of defence-genes. Using resveratrol synthase and stilbene synthase as examples, it can be show that pharmacological

Results

manipulation of microtubules could induce gene expression in the absence of elicitor. These results indicated that cytoskeleton acts upstream of gene expression in the response to the Harpin elicitor in grapevine.

4 Discussion

The cytoskeleton responds actively to numerous signals by reorientation, bundling/debundling, and disassembly/assembly. The scope of this work was to elucidate, whether these cytoskeletal phenomena are just down-stream responses, or whether the cytoskeleton participates in signal perception, regulation, or signal exchange. I have investigated this in two models: light-regulated synchrony of cell division as a response that is triggered by an abiotic stimulus, and elicitor-triggered defence as response to a biotic signal.

4.1 Synchronized cell division is under the control of polar auxin transport

As a consequence of their sessile lifestyle, plants have to respond to environmental cues and adjust their development in order to adapt to their surroundings. Light is important for plants, not only as an energy source of photosynthesis but also as one of the most central signals. The open morphogenesis characterized by flexibility of plants requires that pattern formation must be able to cope with the continuous expansion of the through reiterative addition of new elements (for a review, see Nick, 2006). The development of cell files which is composed of cells, the basic units of plants, can serve as a model of development on the whole plant level.

In previous work, tobacco cell lines such as VBI-0 (Campanoni et al., 2003) and BY-2 (Maisch and Nick, 2007) have been used as model systems to study cellular aspects of reiterative pattern formation, and polar flux of auxin was indentified as a synchronizer of cell division in these cell lines. This synchrony is disrupted either by inhibiting auxin efflux through NPA or by inducing bundling of actin

filaments through overexpression of talin, an actin-bundling protein. An interesting aspect would be to understand how light influences pattern formation of tobacco. However, the lack of light responses in these cell lines stimulated the search for new cell lines that combine patterning with responsiveness to light. Clonal descendants of the VBI-0 line were therefore screened for auxin-autonomous growth and responsiveness to light manifested by chlorophyll synthesis. The cell line VBI-3, isolated from this screen, has preserved the division pattern of its ancestral line VBI-0. For instance, cell division follows a similar time course, and the predominance of even-numbered files as a manifestation of synchronized cell division is maintained (Fig. 3.1). However, in contrast to the ancestral line VBI-0, division activity and division synchrony of VBI-3 are independent of exogenous auxin.

4.1.1 Light reverses the effect of NPA on synchronized division

The synchrony of division can be disrupted by NPA, suggesting that polar auxin transport is responsible for the division synchrony (Fig. 3.2). When time courses of cell density in the dark versus the light in the absence or presence of NPA (Fig. 3.2D) were scored, it was observed, as expected, that the progress of cell division progressed somewhat slower after treatment with NPA. However, there was an interesting difference between dark and light: in the dark, NPA caused only a minor delay, and the culture reached the same final density of cell files (NB: the average number of cells per individual file was basically unchanged). In the light, the delay was much more pronounced (again, the average number of cells per individual file was not much changed). The division synchrony could be restored by light or by exogenous IAA. When the light effect was analysed further by administering different light qualities at equal fluence rates (Fig. 3.3), continuous far-red light was found to rescue the synchrony most efficiently, followed by blue light, whereas red light was least effective.

4.1.2 Phytochrome A is involved in the light dependent rescue

Among the plant photoreceptors, only the phytochromes are able to sense far-red light. Plant phytochromes are synthesized in the inactive P_r form and, upon exposure to light, are transformed into the active P_{fr} form. Since P_r absorbs red light and P_{fr} preferentially absorbs far-red light, it would be expected that phytochrome-triggered responses are induced by red light (establishing a high photoequilibrium of active P_{fr} in relation to total phytochrome) and inactivated by far-red light. In fact, this has been the operational criterion to define a phytochrome-dependent light response (Butler, 1959). Phytochrome is encoded by a small gene family with five members in Arabidopsis (PHYA to PHYE) or three members (PHYA to PHYC) in rice. One member, so-called PHYA, decays upon irradiation, whereas the other members (PHYB and PHYC) are synthesized constitutively, and do not decay upon irradiation with light so that they are terminologically separated as 'stable' from the 'labile' phytochromes (Furuya, 1993).

The photodestruction of PHYA has the consequence that continuous red light will be less effective in triggering a phytochrome-dependent response, because more PHYA per time unit will be shifted into the P_{fr} than can be utilized for signalling. This excess P_{fr} will then undergo decay and therefore is not available for signalling. In contrast, continuous far-red light will only produce the P_{fr} necessary to trigger signalling, avoiding excess P_{fr} , such that the proportion of P_{fr} undergoing decay is negligible in relation to that channelled to signalling. Therefore, for continuous irradiation, far-red light will be more efficient than red light. This so-called far-red-dependent high irradiation response is specific for photolabile (PHYA) species, but is not observed for responses triggered by the light-stable phytochromes (Kneissl et al., 2008). A similar high irradiation response is expected for other light qualities that will establish a low

Discussion

photoequilibrium, for instance blue light. Therefore, -dependent responses are expected to be most efficiently induced by continuous far-red light and blue light, whereas continuous red light should evoke only a weak effect. This is exactly what is observed for the light quality dependence of division synchrony in VBI-3 (Fig. 3.3), consistent with the hypothesis that the responsible photoreceptor is a photolabile () form of phytochrome. It cannot be excluded, however, that a blue light receptor (a cryptochrome) acts in concert with . Bichromatic irradiation with blue light and far-red light establishing different photoequilibria would be required to exclude a cryptochrome activity. However, as the exclusive photoreceptor would be sufficient to explain the observed wavelength dependency of synchrony rescue in VBI-3.

This is not the first example of an interaction between NPA and light. A decade ago, Jensen (1998) reported that NPA inhibited hypocotyl elongation in light dependently. Interestingly, the wavelength dependency was the same as found for division synchrony in VBI-3: continuous far-red light and blue light were most effective, whereas continuous red light had little impact. However, in hypocotyls, NPA was not active in the dark, but requires light to be effective. In contrast, in patterned cell division, NPA is active in the dark, but its activity is alleviated by light. This difference may be related to the fact that hypocotyl elongation is under control of gibberellins, whereas gibberellins have been found not to be effective in suspension cultures of tobacco (Hofmanová , 2008).

Since the synchrony of cell division depends on a polar flux of auxin (manifested as sensitivity of synchrony to the auxin transport inhibitor NPA), and since light can rescue synchrony in the presence of NPA, the light effect must be somehow related to auxin. It should be kept in mind, however, that the effect of auxin fluxes is modified, especially during the first cycles of a developing cell file, by the intrinsic polarity of the progenitor cell (Campanoni , 2003), which becomes manifest, for instance, by the fact that the frequency of three-cell files after treatment with NPA is similar, but does not exceed the frequency for four-cell files.

Discussion

At present, two possible scenarios can be developed to explain the light effect. Light could stabilize the activity of the auxin efflux carrier against inhibition through NPA. From binding studies with different ligands, it has been inferred that the ligand-binding surface of this carrier is multifaceted (Brunn , 1992). It is therefore conceivable that light-dependent factors bind to this surface, and induce conformational changes culminating in a reduced affinity of NPA for this carrier. Alternatively, light could shift the cycling of the auxin efflux carrier towards the active, membrane-bound state in a similar manner to its induction by IAA (Paciorek , 2005). In response to NPA, the actin filaments in VBI-3 are partitioned towards the nucleus and eventually disintegrate (Fig. 3.4), a response which has also been reported for roots of Arabidopsis (Rahman , 2007). Actin filaments participate in the synchronization of cell division in tobacco cell cultures by regulating polar auxin flux (Maisch and Nick, 2007), and, in turn, the organization of actin is regulated by auxin establishing a feedback loop between cellular auxin content, auxin flux, and actin organization. Light could interfere with this feedback loop by stabilizing actin filaments against the disruption through NPA. In fact, phytochrome activation has been shown to alter the organization of actin filaments in epidermal cells of Graminean coleoptiles (Waller and Nick, 1997; Waller , 2002). Experiments are ongoing at present in an attempt to establish transgenic VBI-3 lines expressing the actin-binding domain of plant fimbrin in fusion with green fluorescent protein (GFP) as a tool to follow actin responses to light, auxin, and NPA .

However, there is a much more straightforward model to explain the light effect on division synchrony. The inhibition of division synchrony was alleviated not only by light, but also by exogenous IAA (Fig. 3.2C). This indicates that, upon inhibition of polar auxin transport, it is a decrease of the cellular IAA content which impairs efficient synchronization. Evidence from BY-2 cells expressing the auxin-responsive DR5 promotor driving a GFP reporter in combination with localized release of auxin demonstrates that the terminal cells of a file act as auxin sources that export auxin to their downstream neighbours; treatment with

Discussion

NPA causes a significant decrease of DR5 activity in those downstream cells, indicating that cell-autonomous synthesis is limiting (Kusaka et al., 2009). If light would stimulate the synthesis of IAA, the constraints imposed upon synchronization through the application of NPA would be relieved in the same way as they are relieved when exogenous IAA is added directly. Consistent with this model, the recently published work by Tao et al. (2008) demonstrates that continuous activation of DR5 by white light of a high red/far-red ratio (simulating canopy shading) can induce a novel aminotransferase, TAA1, that catalyses the formation of indole pyruvic acid from tryptophan as the first step of a previously proposed, but uncharacterized, auxin synthetic pathway. If this or a similar auxin synthesis pathway were activated by DR5 in VBI-3, this could explain both why patterning becomes more resistant to NPA and why the light effect can be mimicked by exogenous IAA.

There is, however, an additional, spatial effect to be considered. When time courses of overall cell density were scored (Fig. 3.2D), NPA was observed to cause a general reduction of global cell division activity. This reduction was hardly visible in the dark, but was pronounced upon illumination. This result indicates that in the light not only synchrony, but cell division per se was much more dependent on auxin efflux from the terminal cell into the proximal cells of the file. In other words, auxin synthesis might be more strictly confined to the terminal cell in response to light- as compared with dark-grown cells. In the meantime an approach to test this exciting possibility directly by localized release of auxin from an esterase-resistant caged precursor has been established (Kusaka et al., 2009).

Patterned cell division has been studied in great detail in the root meristem of Arabidopsis, where the pattern can be traced back to early embryogenesis. However, the meristematic pattern of cell division is already established when the root meristem becomes accessible to cell-biological inspection, and it is very difficult, if not impossible, to manipulate these patterns in a fundamental manner.

Thus, root meristems represent a beautiful system to study pattern perpetuation, but for the analysis of pattern induction simpler systems that are less pre-determined might be more appropriate. Suspension lines of tobacco provide such models to study the primordial stages of division patterning and, in general, cellular aspects of cell division. A major drawback of the tobacco suspension cell culture system is the absence of a specific response of patterning to important environmental signals, such as light. The isolation of the VBI-3 cell line overcomes this drawback and allows the investigation of the cellular events that link photomorphogenesis to patterned cell division. To gain insight into the mechanisms driving light-dependent patterning, it is planned to follow the response of cellular auxin content to irradiation. Moreover, in order to be able to address the spatial pattern of auxin abundance in a cell file, transgenic lines that express the auxin-responsive DR5 promoter driving GFP as reporter are presently being generated. In parallel, a novel approach to control the concentration of IAA at cellular or even subcellular resolution with an esterase-resistant caged auxin that can be locally released by spatially confined irradiation has recently been established (Kusaka et al., 2009), and this technique will be used to study patterning in the context of specific transcellular auxin gradients.

4.2 The differences of defense response in resistant and sensitive grapevine species

Life is not easy - this is especially true for plant cells that cannot run away, but have to cope with environmental challenges by adaptation. Pathogen defence represents a specific aspect of this general ability. Whereas the description of plant defence had been dominated by the gene-for-gene concept, during recent years, evolutionary more ancient systems of innate immunity have shifted into attention. When a plant cell is challenged by a pathogen, it responds on two levels: biochemically, by an induction of defence genes leading to the synthesis

of specific secondary metabolites with antibiotic activities, the phytoalexins (for review see Zhao , 2005), and, structurally, by a repolarization of cytoplasmic architecture towards the site of penetration (for review see Schmelzer, 2002).

These responses are triggered, for instance, by the binding of PAMPs, such as bacterial flagellin (Zipfel , 2004), to leucine-rich repeat receptor-like kinases (for review see Morris and Walker, 2003). The activation of the receptor, as a next step, seems to activate ion channels with some evidence for a cross-talk with mechanosensing (Zimmermann , 1997; Gus-Mayer , 1998). These ion fluxes are accompanied by the formation of reactive oxygen species (Nürnberg , 1994; Jabs , 1996), the induction of phytoalexin metabolism, and, in some cases, by programmed cell death (for review see Jones, 2001).

Cytoskeletal reorganization has been identified as an important element of defence responses during innate immunity and is generally interpreted as downstream event in the context of redistributing vesicles containing phytoalexins and cell-wall components towards the penetration site (for reviews see Schmelzer, 2002; Takemoto and Hardham, 2004; Kobayashi and Kobayashi, 2008). To address the question, whether the cytoskeleton, in addition, participates in signal processing, we followed the response to the Harpin elicitor in two cell lines from grapevine genotypes that differed in their microtubule dynamics.

4.2.1 Defence responses triggered by Harpin are more profound and rapid in resistant species

To monitor rapid elicitor responses upstream of gene expression, we used proton influx. Although the biological function of this proton influx is not understood, the resulting alkalization of the external medium can be used as simple readout for quantitative analysis of the cellular response to elicitors (Felix , 1993), and has been employed successfully to investigate the function of Harpin (Wei ,

1992a). As marker for defence-related gene induction we used stilbene synthase (StSy), and resveratrol synthase (RS). Stilbenes, in general, and resveratrol, in particular, have been shown to harbour antifungal activities. In fact, overexpression of stilbene synthase genes in tobacco (Hain , 1993), rice (Stark-Lorenzen , 1997), Kiwi (Kobayashi , 2000), alfalfa (Hipskind and Paiva, 2000), barley (Leckband and Lörz, 1998), a grapevine rootstock (Coutos-Thévenot 2001), and apple (Szankowski , 2003), were found to confer resistance to fungal pathogens.

Both readouts for the elicitor response showed a more sensitive and a more pronounced response of the cell line as compared to cv. 'Pinot Noir' (Figs. 3.5 and 3.12). This was correlated with a more pronounced response of both microtubule fragmentation (Fig. 3.7), and actin bundling (Fig. 3.9). Moreover, by pharmacological manipulation of microtubules, we could partially induce defence genes in the absence of elicitor (Fig. 3.12).

4.2.2 Two grapevine cell line undergo different microtubular disintegration in response to Harpin

The microtubular disintegration in response to Harpin was more pronounced in as compared to cv. 'Pinot Noir', although the higher abundance of deetyrosinated α -tubulin (Fig. 3.7F) and the increased tolerance to oryzalin (Fig. 3.8) indicates that microtubular lifetimes are increased in . Thus, the elimination of microtubules is unlikely to be caused by mere inhibition of microtubule assembly, but probably involves disruption of polymerized microtubules. Such a disruption can be produced, for instance, by so called severing proteins such as plant katanin (Stoppin-Mellet , 2008). Interestingly, microtubule-severing activity of (also employing a type-III effector) has been found to be crucial for intercellular spreading of this pathogen (Yoshida , 2008), and the host response to type III effector was suppressed

by dysfunction of the cytoskeleton (Marois , 2002). Thus, our findings on the Harpin elicitor are consistent with an emerging role of microtubules for the defence response to type-III effectors.

4.3 Differential response of the plant cytoskeleton during the sensing of light and elicitor

The comparison between the cytoskeletal response to light (as abiotic stimulus) versus Harpin (as biotic stimulus) reveals certain common topics, but also some differences:

I could demonstrate for the first time here that light regulates synchronized cell division upstream of auxin (see result part 3.1). As the actin cytoskeleton is known to be a key player in this auxin-transport dependent patterning (Campanoni , 2003), and phytochrome is involved in both synchronized cell division pattern (see result part 3.1.3) and auxin synthesis (Tao , 2008), a first model for the interaction among auxin, microfilament and light is appearing (Fig. 4.1). In this model, microfilaments act as downstream regulators for light induced synchrony of cell division. Since the polarity of auxin transport depends on the degree of actin bundling, which in turn is regulated by auxin, light might control this actin-auxin oscillator (Nick, 2010) by up-regulation of auxin-synthesis genes. During the cellular response to challenge by pathogen or elicitors, the most significant response of microfilaments is bundling. The biological function behind this response and signals involved hereby, remain to be elucidated, but these results indicate that auxin might be involved in a manner that is similar to that in light-dependent patterning. Microfilament-dependent polar auxin transport can affect microtubule orientation, as a result, the axis of cell division and expansion will be under the control of auxin flow as well, but this would not be rather a downstream response, whereas the actin response is clearly located upstream of microtubules.

Discussion

In the response to biotic stimuli, it seems that microtubules rather than actin filaments act upstream. By eliminating microtubules through oryzalin or by inhibiting their dynamics through taxol we could induced the expression of defence genes even in the absence of the Harpin elicitor. This finding complements published evidence accumulates that suggests an interaction between microtubules and mechanosensitive ion channels that are important for the induction of defence responses (Zimmermann, 1997; Gus-Mayer, 1998). When microtubules were disassembled by antimicrotubule agents, both mechano-sensing (Zhou, 2007; Wymer, 1996), and mechanosensitive calcium fluxes (Ding and Pickard, 1993) were affected. Moreover, the control of protoplast volume during the response to hyperosmotic stress relied on microtubule bundling (so called macrotubules, Komis, 2002). In cold sensing, which probably uses changes of membrane fluidity as signal, microtubule dynamics was identified as central component (Abdrakhamanova, 2003). Microtubules might act as negative regulators (sphincters) of ion-channel activity (in case of cold sensing) or, in case of mechano-sensing as stress-focussing elements (susceptors) that collect and convey membrane perturbations to a channel (reviewed in Nick, 2008). In contrast to a sphincter model, stress-focussing would be more efficient with stable microtubules, explaining the increased elicitor responsiveness in over cv 'Pinot Noir'.

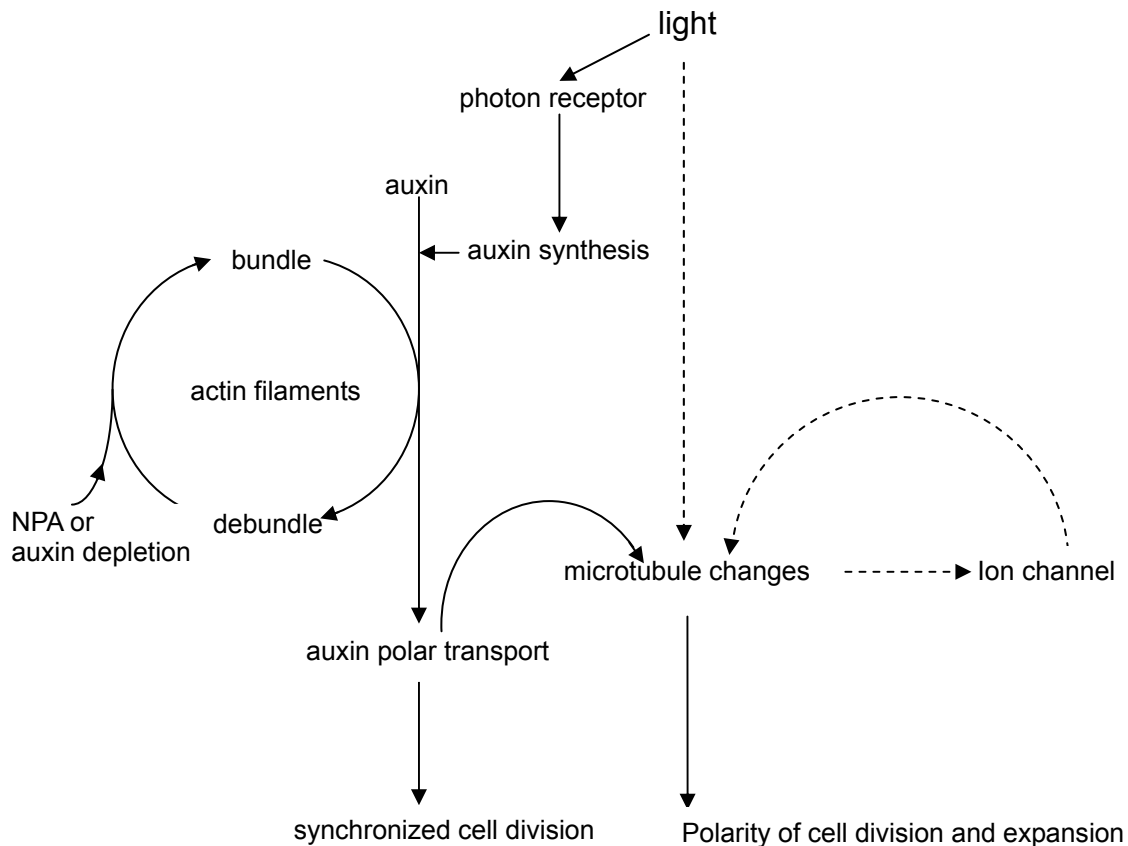


Figure 4.1 Effect of light on cell patterning via cytoskeleton. Solid lines represent the pathway with experimental evidences. The phenomena connected by dashed lines are still lacking of experimental evidence.

4.4 Conclusion

The cytoskeleton has been found to undergo various changes in response to environmental stimuli. They play key roles in both abiotic and biotic signal sensing. In the present work, the cytoskeleton reorganizations in response to light and elicitor were investigated.

The synchronized cell division during the exponential phase of the tobacco cell line VBI-3 was used as model for light induced pattern formation. Here, polar auxin flux dependent on microfilaments can be blocked by NPA. As a consequence, synchronized cell division is disturbed, but both light and

Discussion

exogenous IAA can rescue the impaired pattern. Further investigations have shown that far-red light is most effective in rescuing the interrupted pattern which indicates that light restores this pattern through induction of auxin synthesis.

The elicitor Harpin can trigger on various defence responses such as ion flux, ROS, cellulose papilla formation, defence gene expression and phytoalexin synthesis. Here we mainly concentrated on the functions of the cytoskeletons. Harpin can induce extracellular alkalization which is one of the earliest defence responses. This response is more profound and faster in *Vitis rotundifolia* than cv. 'Pinot Noir'. We analyzed this phenomenon quantitatively and found that the effective concentrations were much lower in *V. rotundifolia*. Microfilaments formed bundles after being challenged by Harpin, and these bundled microfilaments facilitate nuclear movement towards to penetration site of the pathogen, which is closely related to papilla formation (Schmelzer, 2002).

Contrarily, microtubules underwent disintegration in both grapevine cell lines. However, the mechanisms of disintegration differed. Higher level of deetyrosinated tubulin and resistance to oryzalin in *V. rotundifolia* indicates that disintegration is brought about by disruption of polymerized microtubules rather than by microtubule disassembly.

The activation of defence genes by the elicitor is faster and more profound in *V. rotundifolia*.

The expressions of the defence genes can be triggered partially in the absence of elicitor by inhibitors of cytoskeleton assembly or disassembly. Thus, it is not only the presence of microtubules, but also their dynamics that can regulate defence gene expression. Based on these results, we conclude that microtubules act upstream in the regulation of elicitor-triggered gene expression.

5 Outlook

(1) Patterned cell division has been studied in great detail in the root meristem of *Arabidopsis thaliana*, where the pattern can be traced back to early embryogenesis. However, the meristematic pattern of cell division is already established when the root meristem becomes accessible to cell-biological inspection, and it is very difficult, if not impossible, to manipulate these patterns in a fundamental manner. Thus, root meristems represent a beautiful system to study pattern perpetuation, but for the analysis of pattern induction simpler systems that are less pre-determined might be more appropriate. Suspension lines of tobacco provide such models to study the primordial stages of division patterning and, in general, cellular aspects of cell division. A major drawback of the tobacco suspension system is the absence of a specific response of patterning to important environmental signals, such as light. The isolation of the VBI-3 cell line overcomes this drawback and allows the investigation of the cellular events that link photomorphogenesis to patterned cell division. To gain insight into the mechanisms driving light-dependent patterning, it is planned to follow the response of cellular auxin content to irradiation. Moreover, in order to be able to address the spatial pattern of auxin abundance in a cell file, transgenic lines that express the auxin-responsive DR5 promoter driving GFP as reporter have been generated. In parallel, a novel approach to control the concentration of IAA at cellular or even subcellular resolution with an esterase-resistant caged auxin that can be locally released by spatially confined irradiation has recently been established (Kusaka et al., 2009), and this technique will be used to study patterning in the context of specific transcellular auxin gradients.

(2) Elicitors, which can trigger host resistance, are valuable tools to partially substitute pesticides. The corresponding receptors at the plasma membrane are gradually emerging (e.g. Zipfel et al., 2003). Type-III secretion effectors that

Outlook

permeate the membrane and enter the cytoplasm would circumvent recognition by plasma-membrane localized receptors. However, since the cytoskeleton seems to be a major target for this type of effector proteins, and since the cytoskeleton acts as regulator of mechanosensitive ion channels that can trigger plant defence, the intracellular interaction between effector and cytoskeleton might be sensed by the host cell independently of (or in parallel with) recognition at the plasma membrane. Future work should therefore try, on the one hand, to elucidate the molecular interaction between microtubules and ion channels, and the molecular interaction between type-III effectors and the cytoskeleton on the other. To dissect the chain of events, it will not only be necessary to follow cytoskeletal responses using appropriate fluorescent marker lines in grapevine, but also to use microfluidics in order to administer the elicitor to specific locations of the cell to investigate the spatial patterns of cellular responses.

Acknowledgements

I express my sincerely respects to Prof. Dr. Peter Nick for his supervision, precious suggestions and for giving me the opportunity to learn about the interaction between cytoskeleton and environmental stimuli which opened my eyes on a new and interesting field.

I am grateful to Dr. Jan Petrášek (Institute of Experimental Botany, Czech Academy of Science) for generation the cell line VBI-3. I want to specially thank Ms Xiaoli Chang for her nice work in the part of gene expression.

I sincerely express my gratitude to Prof. Dr. Tilman Lampart, Dr. Michael Riemann, Dr. Jan Maisch, Dr. Lars Wegner, Dr. Petra Hohenberger, Aleksandra Jovanovic, Kai Eggenberger Gregor Rottwinkel, Nicole Frey, Ernst Heene and Sabine Purper for their constructive suggestions and technical assistance.

I thank again for Dr. Micheal Riemann, Dr. Jan Maisch, Qiong Liu, and Aleksandra Jovanovic for critical reading of my thesis.

I take the opportunity to thank all the colleagues in Botanik institute 1 for the comfortable working atmosphere during the last three years.

Finally, I express my heartfelt love to my parents and my wife Dr. Xuefei Jiang for their encouraging, inspiration, support, and to my sweet heart son Jiangnan Qiao.

Literature cited

Abdrakhamanova A, Wang QY, Khokhlova L, Nick P. 2003. Is microtubule assembly a trigger for cold acclimation? **44**, 676-686.

Aderem A. 1992. Signal transduction and the actin cytoskeleton: the roles of MARCKS and profilin. **17**, 438-443.

Arlat M, Van Gijsegem F, Huet JC, Pernollet JC, Boucher CA. 1994. PopA1, a protein which induces a hypersensitivity-like response on specific *Petunia* genotypes, is secreted via the Hrp pathway of *Pseudomonas solanacearum*. **13**, 543-553.

Baluška F, Jasik J, Edelmann HG, Salajová T, Volkmann D. 2001. Latrunculin B-Induced plant dwarfism: plant cell elongation is F-actin-dependent. **231**, 113–124.

Baskin TI, Wilson JE, Cork A, Williamson RE. 1994. Morphology and microtubule organization in *Arabidopsis* roots exposed to oryzalin or taxol. **35**, 935–942.

Belhadj A, Telef N, Saigne C, Cluzet S, Barrieu F, Hamdi S, Mérillon JM. 2008. Effect of methyl jasmonate in combination with carbohydrates on gene expression of PR proteins, stilbene and anthocyanin accumulation in grapevine cell cultures. **46**, 493–499.

Berghöfer T, Eing C, Flickinger B, Petra Hohenberger P, Wegner LH, Frey W, Nick P. 2009. Nanosecond electric pulses trigger actin responses in plant cells. **387**, 590-595.

Binet MN, Humbert C, Lecourieux D, Vantard M, Pugin A. 2001. Disruption of microtubular cytoskeleton induced by cryptogein, an elicitor of hypersensitive response in tobacco cells. **125**, 564–572.

Blakeslee JJ, Peer WA, Murphy AS. 2005. Auxin transport. **8**, 494-500.

Brunn SA, Muday GK, Haworth P. 1992. Auxin transport and the interaction of phytohormones. **98**, 101-107.

Literature cited

Butler WL, Norris KH, Siegelman HW, Hendricks SB. 1959. Detection, assay, and preliminary purification of the pigment controlling photoresponsive development of plants.

45, 1703-1708.

Campanoni P, Blasius B, Nick P. 2003. Auxin transport synchronizes the pattern of cell division in a tobacco cell line.

133, 1251-1260.

Dangl, JL, Jones JD. 2001. Plant pathogens and integrated defence responses to infection.

411, 826–833.

Dantán-González E, Rosenstein Y, Quinto C, Sánchez F. 2001. Actin monoubiquitylation is induced in plants in response to pathogens and symbionts.

14, 1267-1273.

Davis KR, Lyon GD, Darvill A, Albersheim P. 1984. Host-pathogen interactions.

74, 52-60.

Desikan R, Reynolds A, Hancock JT, Neill SJ. 1998. Harpin and hydrogen peroxide both initiate programmed cell death but have differential effects on defence gene expression in

suspension cultures. **330**, 115-120.

Dhonukshe P, Grigoriev I, Fischer R, Tominaga M, Robinson DG, Hašek J, Paciorek T, Petrašek J, Seifertová D, Tejos R, Meisel LA, Zažímalová E, Gadella TWJ, Stierhof YD, Ueda T, Oiwa K, Akhmanova A, Brocke R, Spang A, Friml J. 2008. Auxin transport inhibitors impair vesicle motility and actin cytoskeleton dynamics in diverse eukaryotes.

105, 4489-4494.

Duckett CM and Lloyd CW. 1994. Gibberellic acid-induced microtubule orientation in dwarf peas is accompanied by rapid modification of an α -tubulinisotype.

5, 363-372.

Durso NA and Cyr RJ. 1994. A calmodulin-sensitive interaction between microtubules and a higher plant homolog of elongation factor 1a.

6, 893-905.

Eggenberger K, Merkulov A, Darbandi M, Nann T, Nick P. 2007. Direct Immunofluorescence of Plant Microtubules Based on Semiconductor Nanocrystals. **18**, 1879-1886.

Eun SO, Lee Y. 1997. Actin filaments of guard cells are reorganized in response to light and

Literature cited

- abscisic acid. **115**, 1491-1498.
- Felix G, Duran J, Volko S, Boller T.** 1999. Plants have a sensitive perception system for the most conserved domain of bacterial flagellin. **18**, 265-276.
- Felix G, Regenass M, Boller T.** 1993. Specific perception of subnanomolar concentrations of chitin fragments by tomato cells. Induction of extracellular alkalization, changes in protein phosphorylation, and establishment of a refractory state. **4**, 307-316.
- Fischer K and Schopfer P.** 1998. Physical strain-mediated microtubule reorientation in the epidermis of gravitropically or phototropically stimulated maize coleoptiles. **15**, 119-123.
- Freytag S, Arabatzis N, Hahlbrock Klaus, Schmelzer E.** 1993. Reversible cytoplasmic rearrangements precede wall apposition, hypersensitive cell death and defense-related gene activation in potato/*Phytophthora infestans* interactions. **194**, 123-135.
- Furuya M.** 1993. Phytochromes: Their molecular species, gene families, and functions. **44**, 617-645.
- Gus-Mayer S, Naton B, Hahlbrock K, Schmelzer E.** 1998. Local mechanical stimulation induces components of the pathogen defense response in parsley. **95**, 8398-8403.
- Hadwiger LA, Beckmann JM.** 1980. Chitosan as a component of Pea-*Fusarium solani* interactions. **66**, 205-211.
- Hammond JW, Cai D and Verhey KJ.** 2008. Tubulin modifications and their cellular functions. **20**, 71-76.
- Hawes CR and Satiat-Jeunemaitre B.** 2001. Trekking along the Cytoskeleton. **125**, 119-122.
- He SY, Huang HC, Collmer A.** 1993. *Pseudomonas syringae* pv. *syringae* harpinPss: a protein that is secreted via the Hrp pathway and elicits the hypersensitive response in plants. **73**, 1255-1266.
- Heath IB.** 1974. A unified hypothesis for the role of membrane bound enzyme complexes and microtubules in plant cell wall synthesis. **48**, 445-449.

Literature cited

- Heath MC.** 2000. Nonhost resistance and nonspecific plant defenses. **3**, 315-319.
- Heller R.** 1953. Studies on the mineral nutrition of in vitro plant tissue cultures (in French). **14**, 1-223.
- Hepler PK, Vidali L, Cheung AY.** 2001. Polarized cell growth in higher plants. **17**, 159–187.
- Hertel R, Friedrich U.** 1973. Abhängigkeit der geotropischen Krümmung der Chara-Rhizoide von der Zentrifugalbeschleunigung. *fl* **70**, 173–184.
- Herth W.** 1980. Calcofluor white and Congo red inhibit chitin microfibril assembly of *Poterioochromonas*: Evidence for a gap between polymerization and microfibril formation. **87**, 442-450.
- Hicke L.** 2001. Protein regulation by monoubiquitin. **2**, 195-201.
- Higaki T, Goh T, Hayashi T, Kutsuna N, Kadota Y, Hasezawa S, Sano T, Kuchitsu K.** 2007. Elicitor-Induced cytoskeletal rearrangement relates to vacuolar dynamics and execution of cell death: imaging of hypersensitive cell death in tobacco BY-2 cells. **48**, 1414-1425.
- Himmelspach R and Nick P.** 2001. Gravitropic microtubule reorientation can be uncoupled from growth. **212**, 184-189.
- Hoch HC, Staples RC, Whitehead B, Comeau J, Wolf ED.** 1987. Signaling for growth orientation and cell differentiation by surface topography in . **234**, 1659-1662.
- Hofmannová J, Schwarzerová K, Havelková L, Bořiková P, Petrašek J, Opatrný Z.** 2008. A novel, cellulose synthesis inhibitory action of ancymidol impairs plant cell expansion. **59**, 3963-3974.
- Horst WJ, SACHMOHL n, Kollmeier M, baluška F, Sivagura M.** 1999. Dose aluminium inhibit root growth through the interaction with the cell wall-plasma membrane-cytoskeleton continuum? **215**, 163-174.
- Hwang JU, Lee Y.** 2001. Abscisic acid-induced actin reorganization in guard cells of dayflower is

Literature cited

mediated by cytosolic calcium levels and by protein kinase and protein phosphatase activities.
125, 2120-2128.

Jensen PJ, Hangarter RP, Estelle M. 1998. Auxin transport is required for hypocotyl elongation in light-grown but not dark-grown Arabidopsis. **116**, 455-462.

Jovanović AM, Durst S, Nick P. 2010. Plant cell division is specifically affected by nitrotyrosine. **61**, 901–909.

Jürges G, Kassemeyer HH, Dürrenberger M, Düggelin M, Nick P. 2009. The mode of interaction between *Vitis* and *Plasmopara viticola* Berk. & Curt. Ex de Bary depends on the host species. **11**, 886-898.

Kagawa T, Sakai T, Suetsugu N, Oikawa K, Ishiguro S, Kato T, Tabata S, Okada K, Wada M. 2001. Arabidopsis NPL1: A phototropin homologue controlling the chloroplast high-light avoidance response. **291**, 2138-2141.

Ketelaar T, Faivre-Moskalenko C, Esseling JJ, de Ruijter NC, Grierson CS, Dogterom M, Emons AM. 2002. Positioning of nuclei in Arabidopsis root hairs: An actin-regulated process of tip growth. **14**, 2941–2955.

Kilmartin JV, Wright B, Milstein C. 1982. Rat monoclonal antitubulin antibodies derived by using a new non-secreting rat cell line. **93**, 576-582.

Kneissl J, Shinomura T, Furuya M, Bolle C. 2008. A rice phytochrome A in Arabidopsis: The role of the N-terminus under red and far-red light. **1**, 84-102.

Knight MR, Campbell AK, Smith SM, Trewavas AJ. 1991. Transgenic plant aequorin reports the effects of touch and cold-shock and elicitors on cytoplasmic calcium. **352**, 524-526.

Kobayashi I, Kobayashi Y. 2008. Microtubules and Pathogen Defence. In Nick P, ed, Plant Cell Monogr: Plant Microtubules. Springer-Verlag, Berlin, pp 121-140.

Kobayashi Y, Kobayashi I, Funaki Y, Fujimoto S, Takemoto T and Kunoh H. 1997. Dynamic reorganization of microfilaments and microtubules is necessary for the expression of non-host resistance in barley coleoptile cells. **11**, 525-537.

Kobayashi Y, Yamada M, Kobayashi I, Kunoh H. 1997. Actin microfilaments are required for the expression of nonhost resistance in higher plants. **38**, 725-733.

Literature cited

- Komis G, Apostolakos P, Galatis B.** 2002. Hyperosmotic stress-induced actin filament reorganization in leaf cell of *Chlorophyton comosum*. **375**, 1699-1710.
- Kortekamp A.** 2006. Expression analysis of defence-related genes in grapevine leaves after inoculation with a host and a non-host pathogen. *Plant Physiology and Biochemistry* **44**, 58-67.
- Kreis TE.** 1987. Microtubules containing de-tyrosinylated tubulin are less dynamic. **6**, 2597-2606.
- Kusaka N, Maisch J, Nick P, Hayashi KI, Nozaki H.** 2009. Manipulation of Intercellular Auxin in a Single Cell by Light with Esterase-Resistant Caged Auxins. **10**, 2195-2202.
- Kutschera U, Bergfeld R, Schopfer P.** 1987. Cooperation of epidermal and inner tissues in auxin-mediated growth of maize coleoptiles. **170**, 168-180
- Lappalainen P, Fedorov EV, Fedorov AA, Almo SC, Drubin DG.** 1997. Essential functions and actin-binding surfaces of yeast cofilin revealed by systematic mutagenesis. **16**, 5520-5530
- Lee SC, West C.** 1981. Polygalacturonase from *Rhizopus stolonifer*, an elicitor of chitinase synthetase activity in castor bean (*Ricinus communis* L) seedlings. **67**, 633-639
- Lin R, Ding L, Casola C, Ripoll DR, Feschotte C, Wang H.** 2007. Transposase-Derived factors regulate light signal in *Arabidopsis*. **318**, 1302-1305.
- Maisch J, Fišerová J, Fischer L, Nick P.** 2009. Tobacco Arp3 is localized to actin-nucleating sites in vivo. **60**, 603-614.
- Maisch J, Nick P.** 2007. Actin is involved in auxin-dependent patterning. **143**, 1695-1704
- Mathur J and Chua NH.** 2000. Microtubule stabilization leads to growth reorientation in *Arabidopsis* trichomes. **12**, 465-477
- McClinton RS, Sung ZR.** 1997. Organization of cortical microtubules at the plasma membrane in *Arabidopsis*. **201**, 252-260
- McGough A, Chiu W.** 1999. ADF/cofilin weakens lateral contacts in the actin filament.

Literature cited

291, 513–519

- Mohr H.** 1972. Lectures on Photomorphogenesis. Berlin: Heidelberg: Springer Press, 1--12.
- Morris DA.** 2000. Transmembrane auxin carrier systems-dynamic regulators of polar auxin transport. **32**, 161-172.
- Muday GK, Murphy AS.** 2002. An emerging model of auxin transport regulation. **14**, 293-299.
- Nick P. 1990. Versuch über Tropismus, Querpolarität, und Microtubuli. Ph.D thesis. Albert-Ludwigs university, Freiburg.
- Nick P.** 1999a. Signals, motors, morphogenesis- the cytoskeleton in plant development. **1**, 169-179.
- Nick P.** 1999b. Control of the response to low temperatures. In Nick P, ed, Plant Cell Monogr: Plant Microtubules. Springer-Verlag, Berlin, pp121-135.
- Nick P.** 2000. Control of response to low temperature. In Nick P, ed, Plant Cell Monogr: Plant Microtubules. Springer-Verlag, Berlin, pp 121-136.
- Nick P.** 2006. Noise yields order – auxin, actin, and polar patterning. **8**, 360-370.
- Nick P.** 2008a. Microtubules as Sensors for Abiotic Stimuli. In Nick P, ed, Plant Cell Monogr: Plant Microtubules. Springer-Verlag, Berlin, pp 175-203.
- Nick P.** 2008b. Microtubules and the control of cell axis. In Nick P, ed, Plant Cell Monogr: Plant Microtubules. Springer-Verlag, Berlin, pp 3-46.
- Nick P.** 2010. Probing the actin-auxin oscillator. **5**, 94-98.
- Nick P, Bergfeld R, Schaefer E, Schopfer P.** 1990. Unilateral reorientation of microtubules at the outer epicermal wall during photo- and gravitropic curvature of maize coleoptiles and sunflower hypocotyls. **181**, 162-168.
- Nick P, Ehmann B, Schäfer E.** 1993. Cell communication, stochastic cell responses, and anthocyanin pattern in mustard cotyledons. **5**, 541-552.
- Nick P, Heuing A, Ehmann B.** 2000. Plant chaperonins: a role in microtubule-dependent

Literature cited

- wall-formation? **211**, 234-244.
- Nick P, Lambert AM, Vantard M.** 1995. A microtubule-associated protein in maize is expressed during phytochrome-induced cell elongation. **8**, 835–844.
- Nürnberg T, Brunner F.** 2002. Innate immunity in plants and animals: emerging parallels between the recognition of general elicitors and pathogen-associated molecular patterns. **5**, 1-7.
- Nürnberg T, Nennstiel D, Jabs T, Sacks WR, Hahlbrock K, Scheel D.** 1994. High affinity binding of a fungal oligopeptide elicitor to parsley plasma membranes triggers multiple defense responses. **78**, 449-460.
- Opatrný Z, Opatrná J.** 1976. The specificity of the effect of 2,4-D and NAA on the growth, micromorphology, and occurrence of starch in long-term *Nicotiana tabacum* L. cell strains. **18**, 359-365.
- Ouellet F, Carpentier E, Cope MJ, Monroy AF, Sarhan F.** 2001. Regulation of a wheat actin-depolymerizing factor during cold acclimation. **125**, 360–368.
- Paciorek T, Zažimalová E, Ruthardt N, Petrášek J, Stierhof YD, Kleine-Vehn J, Morris DA, Emans N, Jürgens G, Geldner N, Friml J.** 2005. Auxin inhibits endocytosis and promotes its own efflux from cells. **435**, 1251-1256.
- Palmieri M and Kiss JZ.** 2005. Disruption of the F-actin cytoskeleton limits statolith movement in *Arabidopsis* hypocotyls. **56**, 2539-2550.
- Parker JE, Schulte W, Hahlbrock K, Scheel D.** 1991. An extracellular glycoprotein from *Phytophthora megasperma* f. sp. *glycinea* elicits phytoalexin synthesis in cultured parsley cells and protoplasts. **4**, 19-27.
- Rahman A Bannigan A, Sulaman W, Pechter P, Blancaflor EB, Baskin TI.** 2007. Auxin, actin and growth of the *Arabidopsis thaliana* primary root. **50**, 514-528.
- Reid KE, Olsson N, Schlosser J, Peng F, Lund ST.** 2006. An optimized grapevine RNA isolation procedure and statistical determination of reference genes for real-time RT-PCR during berry development. **6**, 27-37.
- Reinhardt D, Pesce ER, Stieger P, Mandel T, Baltensperger K, Bennett M, Traas J, Friml J,**

Literature cited

- Kuhlemeier C.** 2003. Regulation of phyllotaxis by polar auxin transport. **426**, 255-260.
- Ricci P, Bonnet P, Heut JC, Sallantin M, Beauvais-Cante F, Bruneteau M, Billard V, Michel G, Pernollet JC.** 1989. Structure and activity of proteins from pathogenic fungi *Phytophthora* eliciting necrosis and acquire resistance in tobacco. **183**, 555-563.
- Rothwell GW, Lev-Yadun S.** 2005. Evidence of polar auxin flow in 375 million-year-old fossil wood. **92**, 903-906.
- Seibicke T.** 2002. Untersuchungen zur induzierten Resistenz an *Vitis spec.*. Ph.D. thesis. University of Freiburg.
- Schmelzer E.** 2002. Cell polarization, a crucial process in fungal defence. **7**, 411-415.
- Schwarzerová K, Zelenková S, Nick P, Opatrný Z.** 2002. Aluminum-induced rapid changes in the microtubular cytoskeleton of tobacco cell lines. **43**, 207-216.
- Schwuchow J, Sack FD, Hartmann E.** 1990. Microtubule disruption in gravitropic protonemata of the moss *Ceratodon*. **159**, 60-69.
- Skoufias DA and Wilson L.** 1998. Assembly and colchicine binding characteristics of tubulin with maximally tyrosinated and detyrosinated alpha-tubulins. **351**, 115-122.
- Takemoto D, Hardham AR.** 2002. The cytoskeleton as a regulator and target of biotic interactions in plants. **136**, 3864-3876.
- Tao Y, Ferrer JL, Ljung K, Pojer F, Hong F, Long JA, Li L, Moreno JE, Bowman ME, Ivans LF, Cheng Y, Lim J, Zhao Y, Ballare CL, Sandberg G, Noel JP, Chory J.** 2008. Rapid synthesis of auxin via a new tryptophan-dependent pathway is required for shade avoidance in plants. **133**, 164-176.
- Taylor DP, Leopold AC.** 1992. Offset of gravitropism in maize roots by low temperature. **6**, 75.
- Thomas C, Tholl S, Moes D, Dieterle M, Papuga J, Moreau F, Steinmetz A.** 2009. Actin bundling in plants. **66**, 940-957.

Literature cited

- Thordal-Christensen H.** 2003. Fresh insights into processed of non host resistance. **6**, 351-357.
- Traas J, Bellini C, Nacry P, Kronenberger J, Bouchez D, Caboche M.** 1995. Normal differentiation patterns in plants lacking microtubular preprophase bands. **375**, 676–677.
- Tsuba M, Katagiri C, Takeuchi Y, Takada Y, Yamaoka N.** 2002. Chemical factor of the leaf surface involved in the morphogenesis of *Blumeria graminis*. **60**, 51-57.
- Twell D, Park SK, Lalanne E.** 1998. Asymmetric division and cell-fate determination in developing pollen. **3**, 305-310.
- Van den Berg C, Willensen V, Hage W, Weisbeek P, Scheres B.** 1995. Cell fate in the *Arabidopsis* root meristem is determined by directional signalling. **378**, 62–65.
- Van Breusegam F and Dat JF.** 2006. Reactive oxygen species in plant cell death. **141**, 384–390.
- Vidal S, Eriksson ARB, Montesano M, Dencke J, Palva T.** 1998. Cell wall-degrading enzymes from *Erwinia carotovora* cooperate in the salicylic acid-independent induction of a plant defence response. **11**, 23–32.
- Waller F, Nick P.** 1997. Response of actin microfilaments during phytochrome-controlled growth of maize seedlings. **200**, 154–162.
- Waller F, Riemann M, Nick P.** 2002. A role for actin-driven secretion in auxin-induced growth. **219**, 72–81
- Wasteneys GO.** 2003. Microtubules Show their Sensitive Nature. *Plant and Cell Physiology* **44**, 653–654.
- Wei ZM, Laby RJ, Zumoff CH, Bauer DW, He SY, Collmer A, Beer SV.** 1992a. Harpin, elicitor of the hypersensitive response produced by the plant pathogen *Erwinia amylovora*. **257**, 85-88.
- Wei ZM, Sneath BJ, Beer SV.** 1992b. Expression of *Erwinia amylovora* hrp genes in response to environmental stimuli. **174**, 1875-1882.

Literature cited

- Wiesler B, Wang W, Nick P.** 2002. The stability of cortical microtubules depends on their orientation. **32**, 1023-1032.
- Wymer C, Wymer SA, Cosgrove DJ, Cyr RJ.** 1996. Plant cell growth responds to external forces and the response requires intact microtubules. **110**, 425-430.
- Xu J, Scheres B.** 2005. Cell polarity: ROPing the ends together. **8**, 613-618.
- Yamaguchi T, Yamada A, Hong N, Ogawa T, Ischii T, Shibuya N.** 2000. Differences in the recognition of glucan elicitor signals between rice and soybean: b-Glucan fragments from the rice blast disease fungus *Pyricularia oryzae* that elicit phytoalexin biosynthesis in suspension-cultured rice cells. **12**, 817-826.
- Zimmermann S, Nürnberger, T, Frachisse JM, Wirtz W, Guern J, Hedrich R, Scheel D.** 1997. Receptor-mediated activation of a plant Ca^{2+} -permeable ion channel involved in pathogen defense. **94**, 2751-2755.
- Zipfel C, Robatzek S, Navarro L, Oakeley EJ, Jones JDG, Felix G, Boller T.** 2003. Bacterial disease resistance in *Arabidopsis* through flagellin perception. **428**, 764-767.

Curriculum Vitae

Persönliche Daten

Name	Fei Qiao
Geburtsdatum	25.09.1977 in Shaanxi Province
Nationalität	China
Kontakt	qiaofeixn@gmail.com 0721 608 8927

Ausbildung

seit 05/2008	Promotionsstudium Karlsruher Institut für Technologie (KIT), Institut für Botanik I
9/2000 – 7/2003	Studium Pomology Northwest A&F University, China Abschluss: Master of Agriculture Science
09/1996 – 07/2000	Studium Pomology Northwest A&F University, China Abschluss: Bachelor of Agriculture Science
09/1993 – 07/1996	High school
09/1990 – 07/1993	Middle school
09/1984 – 07/1990	Primary school

Wissenschaftliche Tätigkeiten

seit 05/2008	Wissenschaftlicher Mitarbeiter (Doktorand) Karlsruher Institut für Technologie (KIT) Institut für Botanik I, AG Prof. Nick
07/2003 – 10/2007	Wissenschaftlicher Mitarbeiter und Lehrbeauftragter Horticulture College, Northwest A&F University, China
09/2001 – 07/2003	Masterarbeit Northwest A&F University, China Horticulture College, AG Prof. Chonghui Fan

Curriculum Vitae

Titel der Arbeit: Construction of genetic linkage map by RAPD and ALFP markers on peach

09/1999 – 07/2000

Bachelorarbeit

Northwest A&F University, China
Horticulture College, AG Vice Prof. Yizhen Wan

Titel der Arbeit: The tannin contents of the seed and the berry skin in Chinese wild

Publications:

Qiao F, Petrášek J, Nick P. 2010

Light can rescue auxin-dependent synchrony of cell division in a tobacco cell line.
2010, 61(2): 503-510.

Qiao F, Chang XL, Nick P. (accepted by)

Cytoskeleton contribute to the transcriptional enhancement of plant defensive genes in response to the Hairpin elicitor